

**PRELIMINARY STUDY ON THE EFFECT OF VIBRATION AND
SURFACTANT ON MALAYSIAN COAL FOR CBM STUDY**

By

ROSAN ESA

14192

Dissertation submitted in partial fulfillment of
the requirements of the
Bachelor of Engineering (Hons)
(Petroleum Engineering)

SEPTEMBER 2014

Universiti Teknologi PETRONAS
Bandar Seri Iskandar
31750 Tronoh
Perak Darul Ridzuan

CERTIFICATION OF APPROVAL

**PRELIMINARY STUDY ON THE EFFECT OF VIBRATION AND
SURFACTANT ON MALAYSIAN COAL FOR CBM STUDY**

By

ROSAN ESA

14192

A project dissertation submitted to the

Petroleum Engineering Programme

Universiti Teknologi PETRONAS

In partial fulfillment of the requirement for the

BACHELOR OF ENGINEERING (Hons)

(PETROLEUM ENGINEERING)

Approved by,

(Dr. SALEEM QADIR TUNIO)

UNIVERSITI TEKNOLOGI PETRONAS

TRONOH, PERAK

SEPTEMBER 2014

CERTIFICATION OF ORIGINALITY

This is to certify that I am responsible for the work submitted in this project, that the original work is my own except as specified in the references and acknowledgements, and that the original work contained herein have not been undertaken or done by unspecified sources or persons

(ROSAN ESA)

ABSTRACT

Coalbed Methane (CBM) is unconventional gas reservoir. High volume of gas located in bituminous coal rank. Coalbed Methane reservoir is dual porosity which is fracture and matrix porosity, gas or other liquids situated in the matrix porosity and migrate through the continuous fracture called face cleats or through the discontinuous fracture called butt cleats. The extraction or production can be made in term of desorption of gas from coal. Desorption becomes more difficult when water production presents in the coal has not been produced therefore it hinders the methane desorption or methane stuck in the matrix and also less permeability of coal will create an inconvenience for methane to migrate or flow from matrix and the declination of methane production. These are the encountered problems that coalbed methane need to be stimulated. Therefore this project is to investigate the effect of changes in Malaysian coal sample characteristics in accordance with the important parameters i.e., frequency, surfactant and temperature. Coal samples from Balingian coalfield, Sarawak, Malaysia are tested to investigate the effect of surfactant and different frequencies at specified temperatures at which yield the positive maximum effect called optimum condition. The results indicate that the coal characteristics are improved or increased at optimum condition. Surfactant stimulation yields the enlargement of the pore of the coal sample at higher temperature. Vibration stimulation proves the improvement of coal properties at optimum frequency of 50 Hz for both temperatures of 50 °C and 70 °C. Hopefully this project can bring some new changes in study of the coalbed methane in the future.

ACKNOWLEDGEMENT

First and foremost, I would like to express my utmost gratefulness to Allah SWT for giving me the strength and good health during the completion of my project. Without His blessing, I would not be able to complete my FYP.

I would like to thank FYP committee members in Petroleum Engineering Department, especially FYP coordinator and examiners.

My special thanks goes to my FYP supervisors, Dr. Saleem Qadir Tunio and Dr. Khurram Altaf, who gave me the opportunities to do this project. Thank you for giving me all the guidance, support, advises and passion in teaching me lots of things throughout my studies under your supervision. You are greatly appreciated.

I would like to take this opportunity to thank individuals involved; lecturers, lab technicians and master student, especially Mr.Samsudin, Mr.Zamil and Mr.Imran who helped me a lot during my FYP experiment.

I would like to thank my beloved family for their unconditional love and support. Thank you for the continuous prayers throughout my FYP completion. Without them, I would not be as strong as I am today.

Last but not least, thank you to my fellow friends who motivated me to finish my FYP successfully.

TABLE OF CONTENTS

CERTIFICATION OF APPROVAL	I
CERTIFICATION OF ORIGINALITY	II
ABSTRACT	III
ACKNOWLEDGEMENT	IV
TABLE OF CONTENTS	V
LIST OF FIGURES	VIII
LIST OF TABLES	X
ABBREVIATIONS AND NOMENCLATURES	XI
CHAPTER 1: INTRODUCTION	1
1.1 BACKGROUND OF STUDY	1
1.2 PROBLEM STATEMENT	3
1.3 OBJECTIVES	3
1.4 SCOPE OF STUDY	3
CHAPTER 2: LITERATURE REVIEW	4
2.1 FORMATION OF COAL	4
2.2 FORMATION OF METHANE	5
2.3 COALBED METHANE RESERVOIR	5
2.4 COALBED METHANE PRODUCTION	7
2.5 COALBED METHANE WELL STIMULATION	8
2.5.1 VIBRATION STIMULATION	8

2.5.2 SURFACTANT STIMULATION	10
2.5.3 TEMPERATURE STIMULATION	11
CHAPTER 3: METHODOLOGY	13
3.1 CORRELATION BETWEEN METHODS AND OBJECTIVES	13
3.2 MATERIALS	13
3.3 EXPERIMENTAL APPARATUS	13
3.4 CONTROL – CONSTRAINTS – CONSTANT	15
3.5 EXPERIMENTAL PROCEDURES/ PROJECT ACTIVITIES	15
3.5.1 COAL SAMPLES PREPARATION	15
3.5.2 EFFECT OF TEMPERATURES	16
3.5.3 EFFECT OF SURFACTANT STIMULATION	17
3.5.4 EFFECT OF VIBRATION STIMULATION	18
3.6 RESEARCH METHODOLOGY	20
3.7 KEY MILESTONES	21
3.7.1 FINAL YEAR PROJECT I	21
3.7.2 FINAL YEAR PROJECT II	21
3.7.3 EXPERIMENTS KEY MILESTONES	21
3.8 GANTT CHART	22
3.8.1 FINAL YEAR PROJECT I	22
3.8.2 FINAL YEAR PROJECT II	23
3.8.3 OVERALL EXPERIMENTS AGAINST GANTT CHART	24

CHAPTER 4: RESULTS AND DISCUSSION	25
4.1 EFFECT OF TEMPERATURES ON COAL	25
4.2 EFFECT OF TEMPERATURES ON POROSITY AND PERMEABILITY	26
4.3 EFFECT OF SURFACTANT STIMULATION ON COAL	27
4.4 EFFECT OF SURFACTANT STIMULATION ON POROSITY AND PERMEABILITY	28
4.5 EFFECT OF VIBRATION STIMULATION ON COAL	29
4.6 EFFECT OF VIBRATION STIMULATION ON POROSITY AND PERMEABILITY	30
4.7 SAMPLE COMPRESSIBILITY	32
4.8 DENSITY CALCULATIONS	34
CHAPTER 5: CONCLUSION AND RECOMMENDATIONS	35
REFERENCES	36
APPENDICES	40

LIST OF FIGURES

Figure 2.1: Coal rank formation	4
Figure2.2: (a) Methane desorption stages, (b) the natural fractures of the coal	6
Figure2.3: Langmuir Isotherm	7
Figure 2.4: Production cycle of CBM	8
Figure 2.5: Methane hydrate formation rate without SDS and different SDS concentrations in 4.17 mol water	11
Figure 2.6: The PD as a function of water pressure at constant temperature 25 degree Celsius and function of water temperature at constant 8.0 MPa	12
Figure 3.1: Containers	13
Figure 3.2: Zip lock bags & Al foils	13
Figure 3.3: Hammer & Cutting tools	14
Figure 3.4: Density test set	14
Figure 3.5: Mercury Porosimeter	14
Figure 3.6: Beakers	14
Figure 3.7: Vibration Shaker setup	14
Figure 3.8: Oven	14
Figure: 3.9: Density test setup	16
Figure 3.10: Maintain the temperature of the coal samples	17
Figure 3.11: Dipping sample in the Sodium Lauryl Sulfate surfactant	17
Figure 3.12: The coal sample was stuck on the plate of vibration shaker	18
Figure 3.13: Research methodology	20

Figure 3.14: Project key milestone for FYP1	21
Figure 3.15: Project key milestone for FYP2	21
Figure 3.16: Experiments Key Milestones for FYP2	21
Figure 4.1: Coal pores curves after effect of temperatures	26
Figure 4.2: Porosity&permeability bar charts after effect of temperatures	27
Figure 4.3: Coal pores curves after effect of surfactant stimulation	28
Figure 4.4: Porosity&permeability bar charts after effect of surfactant stimulation	29
Figure 4.5: Coal pores curves after effect of vibration stimulation	30
Figure 4.6: Porosity&permeability bar charts after effect of vibration stimulation	31
Figure 4.7: Compressibility and permeability curves after stimulations	32

LIST OF TABLES

Table 2.1: Permeability at different frequencies and amplitudes.	9
Table 2.2: Dewatering period at different frequencies and amplitudes	9
Table 3.1: Correlation between the objectives and methodology	13
Table 3.2: Control, constraints and constants in experiment	15
Table 3.3: Gantt chart for Final Year Project 1	22
Table 3.4: Gantt chart for Final Year Project 2	23
Table 3.5: Gantt chart of overall experiments for Final Year Project 2	24
Table 4.1: Coal pores properties after effect of temperatures	25
Table 4.2: Porosity&Permeability results after effect of temperatures	26
Table 4.3: Coal pores properties after effect of surfactant stimulation	27
Table 4.4: Porosity&permeability results after effect of surfactant stimulation	28
Table 4.5: Coal pores properties after effect of vibration stimulation	29
Table 4.6: Porosity&permeability results after effect of vibration stimulation	30
Table 4.7: Compressibility results after stimulation effects	32
Table 4.8: Results of density measurement experiment	34

ABBREVIATIONS AND NOMENCLATURES

Mode	Abbreviation	Full name
Unit	[A]	Weight in air (gram)
	[B]	Weight in water (gram)
	°C	Degree Celsius
	mD	Millidarcy
	mV	Millivolt
	ml	Milli liter
	mg	Milli gram
	g/cm^3	Gram per cubic centimeter
	m/s^2	Meter per second squared
	mm^3/g	Cubic millimeter per gram
	m^2/g	Square meter per gram
	μm^2	Micro meter squared
	1/MPa	One over mega Pascal
	g	Gram
	SI	International system of units
Chemical	OMC 854	Ordered mesoporous carbons
	SDS	Sodium dodecyl sulfate
	SLS	Sodium lauryl sulfate
Sample	S_{base}	Sample at base case
	S_A	Sample A
	S_B	Sample B
	S_C	Sample C
	S_O	Sample O
	S_1	Sample 1
	S_2	Sample 2
	S_3	Sample 3
	S_4	Sample 4
S_5	Sample 5	

	S_6	Sample 6
	S_7	Sample 7
	S_8	Sample 8
Jargon	CBM	Coalbed methane
	NGH	Natural gas hydrate
	PD	Percentage desorption
	PSD	Pore size distribution

CHAPTER 1

INTRODUCTION

1.1 Background of study

Energy is critically needed in term of development. The demand is always tremendously high with depleting in natural gas resources, particularly in the developing country like Malaysia. To supply the high demand with the scarce resources, Unconventional gas resource like coal (new alternative), cleaner and more environmental friendly energy is required. In 1851, coal mining in Malaysia had started. Recently the volume of Malaysian coal is 1050 million tons with coal rank from lignite to anthracite. The coal resources are found mostly in Sarawak 69%, Sabah 29% and other part 2%. Even though the coal reserve is quite big but the demand for the methane is relatively low, but it is still sufficient to meet its demand (Mohamed & Lee, 2014).

Even though the coalbed methane has not yet been produced officially, the abundant study or research on the exploration, extraction and enhancement of coalbed methane are ongoing, Based on the Preliminary study on gas storage capacity and gas-in-place for CBM potential found out that the coalbed methane in Balingian Coal Field, Sarawak Malaysia yields the good potential prospect for the first time produce coalbed methane in Malaysia (Kong et al, 2011).

Coal is originated from the accumulation of the plant materials called “peat” in the swamp environment as coal was buried deeper. It undergoes coalification process where the peat is transformed to lignite, subbituminous, bituminous to anthracite. Methane is generated by two ways, methanogenic (biogenic) process in which the methane is produced in accordance to the bacteria activity in the fine-grained sediment below hundred meters of seabed and thermogenic process where the methane generation is influenced by the effect of temperature and pressure. Desorption can be stimulated by reducing the pressure or increasing the temperature to allow gas to release as free gas from the coal seam (Alberta Energy, 2013).

The mechanism on how unconventional gas reservoir is trapped in the coal matrix is different from the conventional gas reservoir. For conventional gas reservoir the hydrocarbon gas stored and occupied the void whereas the unconventional gas reservoir, methane is trapped on the surface of matrix by the adsorption in micropores (“Coalbed methane”, 2008). Production of methane can be obtained by decreasing the pore pressure below desorption pressure which is the point where the methane desorbs from coal seam as free gas. Coal should have enough fractures either face cleats or butt cleats for gas and other fluids to flow for production (Schlumberger Glossary).

Coalbed Methane production is obtained by pumping out water “dewatering” to help the methane to desorb from the coal matrix. The cleats volume is larger as water production in CBM reservoir decreases thus increases permeability for gas to flow whereas in conventional gas reservoir the gas production is high during the early stage and steadily declines (Kong et al, 2011).

Permeability is essential parameter which drives methane production from coal. The stimulation methods are needed to accelerate the gas production and improve the rock and fluid properties by all means (Christian & Tutuka, 2009). The most common stimulation method is cased hole completion with hydraulic fracturing applies to all CBM reservoir having permeability less than 100 mD (Ramaswamy, 2007). However there is also new alternative way to stimulate the CBM which is by using acoustic wave (Christian & Tutuka, 2009).

1.2 Problem statement

Methane desorption becomes more difficult when water production presents in the coal has not been produced therefore it hinders the methane desorption or methane stuck in the matrix and also less permeability of coal will create an inconvenience for methane to migrate or flow from matrix. After dewatering stage, the stable production stage of methane continues to produce until it reaches the decline stage which is the stage where methane starts to decline until it becomes uneconomic to produce. Coalbed methane stimulations are needed to improve coalbed methane characteristics, accelerate the water production to desorb the methane and stimulate the coalbed methane to desorb remaining methane in the decline stage.

1.3 Objectives

The main objectives of this project are

- To study the effect of vibration on Malaysian coal samples at specified temperatures in order to enhance and improve coalbed methane characteristics
- To study the effect of surfactant on Malaysian coal samples at specified temperatures in order to enhance and improve coalbed methane characteristics

1.4 Scope of study

Experiment in this project was conducted mainly in laboratory. The scope of study covers the processes in accordance to the objectives.

CHAPTER 2

LITERATURE REVIEW

2.1 Formation of coal

The early stage origin of coal begins in the swamp environment saturated mostly with water. All the plant and flora materials lie on layer by layer due to compaction form peat formation. The deeper sediments deposit the higher the pressure and temperature to lose some gases and water to gradually form soft coal or lignite, the bituminous coal and continue to form anthracite as more gases and water lose and exhaust. Depth of burial is the main driving force rather than time, different coal rank can occur in the same time period therefore the coal rank is not the good parameter to determine the age of origin (Trevor, 1996). Rank of coal indicates the degree of metamorphism or coalification which is the transformation process of organic materials therefore different type of plant materials deposit different degree of coalification and the grade of coal or impurities contained (Miler, 2005). As shown in figure 2.1

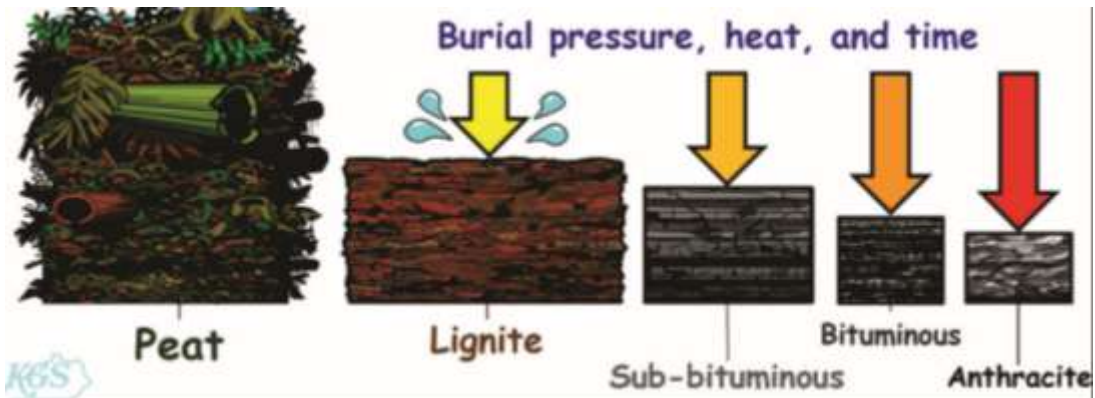


Figure2.1: Coal rank formation (Source: Virginia Energy)

Coal rank class is according to the extent of metamorphism indicating the coal maturation. The higher degree of metamorphism or alternation of coal, the higher carbon content (Miller, 2005). The amount of carbon content increases with respect to the coal rank classes; Peat 52-60%, Lignite 58-77%, Bituminous coal 76-93% and Anthracite 91-93%. The coal rank and its quality are the main factors indicating the capacity of methane desorption from the coal. The absorption in the

peat is relatively low if it closes to surface and gas can produce directly as free gas (Anderson, 2003).

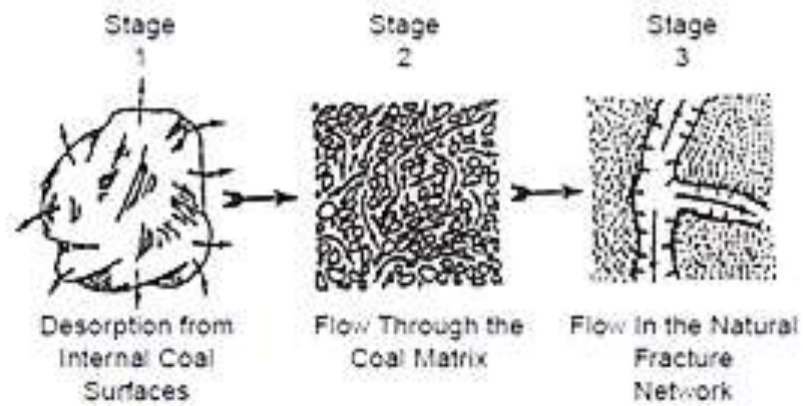
2.2 Formation of methane

Throughout the period of diagenesis process or alteration process of change in sediment to the lithification, the methane is formed by biogenic and thermogenic processes (Kong et al, 2011). Methane is formed from biogenic process by the depleting of oxygen causes the anaerobic oxidation of organic matters at low temperature (Rice & Claypool, 1981). While the thermogenic process, the methane is formed with respect to the increasing temperature with burial depth. At 250 degree fahrenheit the degree of produced methane is much higher than carbon dioxide and methane is generated at maximum temperature of 300 degree fahrenheit (Rightmire, 1984).

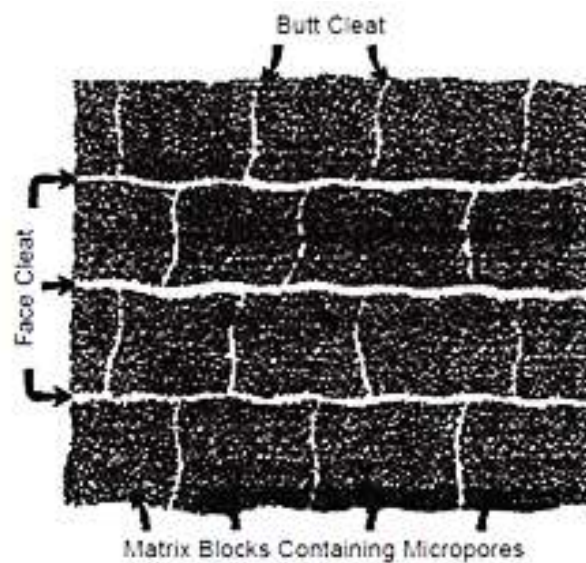
2.3 Coalbed methane reservoir

Coalbed methane reservoir is dual porosity which is fracture and matrix. Matrix acts as the porosity where the methane is adsorbed or stored on the inner coal surface. Fractures act as the path for gas and other liquids to migrate to the wellbore as shown in figure 2.2 (a) (Roger, 1994). The fracture in coal called cleat which is the natural fracture formed by the dehydration or maturing process. Typically there are two types which are continuous fracture called face cleats and discontinuous by the effect of face cleat called butt cleats (Tarek & Nathan, 2012). As shown in figure 2.2 (b).

The mechanism on how the methane is stored on the inner surface of the coal is the adsorption mechanism in which the molecules are attached to the surface. Adsorption is reversible process because the attraction force is weak, for more visualized term, adsorption is like how the magnets adhere on the metal surface unlike the absorption which is irreversible process with high attraction force like how the water is soaked in the sponge (Christian & Tutuka,2009).



(a)



(b)

Figure 2.2: (a) Methane desorption stages, (b) the natural fractures of the coal

(Source: Tarek & Nathan, 2012)

According to the Langmuir adsorption isotherm (figure 2.3), assuming in condensed near liquid state and gas is stored as a single layer on the surface of the coal. Initially the coal is undersaturated where the reservoir pressure is above desorption pressure (1000 psia according to figure 2.3). As the reservoir pressure declines below the desorption pressure (480 psia) undersaturated gas starts to expand and become free gas releasing from the matrix of the coal. The amount of released gas can be calculated by different amount of gas at initial pressure to the amount of gas at final pressure (Christian & Tutuka, 2009).

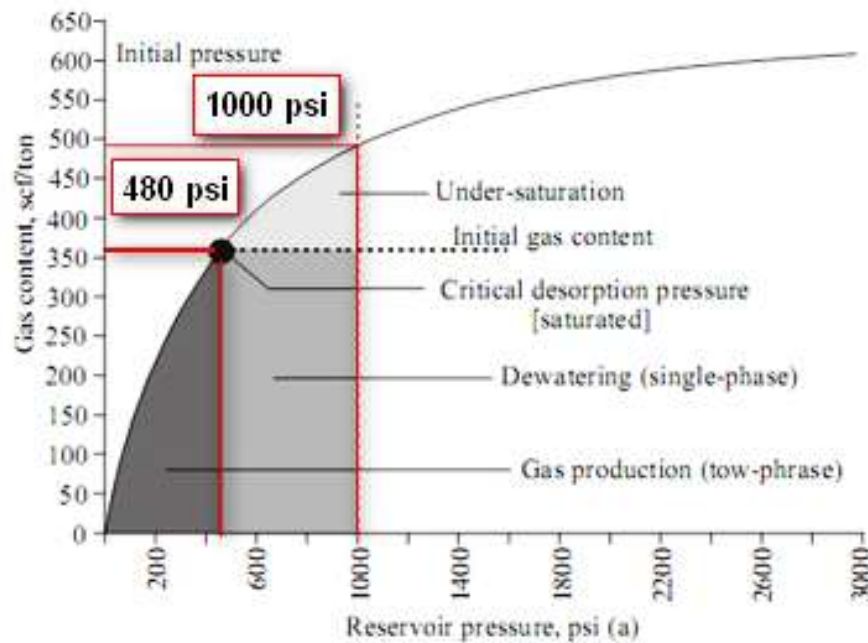


Figure 2.3: Langmuir Isotherm (Tunio et al, 2012)

2.4 Coalbed methane production

For natural cleats with 100% water saturation, water need to be produced so that methane can desorb, move freely through the cleat and diffuse from the coal matrix easily by depressurizing the coal increasing the gas production rate and decline in water production known as “Dewatering”. Production stage, methane continues producing up to the maximum and water production becomes stable and finally declining stage is where methane production declines and becomes uneconomic to produce. (Roadifer & Moore, 2003). As shown in figure 2.4.

According to Lin (2010) widely used method in methane production is primary recovery method by using downhole submersible pump to re move the water production up to reduce reservoir pressure so that methane will desorb from the coal and flow to wellbore. Grattoni et al (2006) also mentioned that most commonly method used in methane production is by depleting the pressure which is simple and effective but not efficient to use when the gas-in-place is less than 50%.

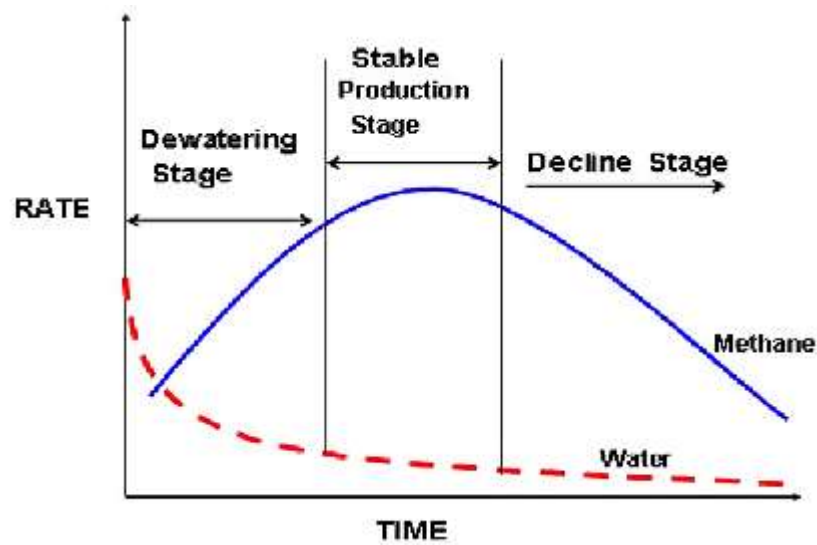


Figure 2.4: Production cycle of CBM (Rogers et al, 1994)

2.5 Coalbed methane well stimulation

The stimulation methods used in this study are vibration and surfactant stimulations to see the effect of changes in frequency, Sodium Lauryl Sulfate and also additional temperature effect.

2.5.1 Vibration stimulation

The experiment was conducted by Christian & Tutuka (2009) using six core samples with permeability range from 0.240-58.85 mD applying the vibration frequency of 15-20 Hz , amplitude 5, 20 and 50 mv to the core samples while injecting the nitrogen gas at 100 psi at overburden pressure of 300 psi. The result of this study found out that, at optimum frequency 10-15 Hz and amplitude around 20mV lead to increase in permeability from 7.35% to 160 % as shown in figure 2.5. The greater the amplitude the greater permeability and the vibration method can reduce dewatering period as shown in figure 2.6. As the greater fracture permeability more easily for fluid to flow and therefore reservoir productivity is increased.

Ariadji (2005) described the mechanism of vibration that the agitation due to vibration helps to connect the non-connective porosity, reduce the surface tension, reduce the tortuosity thus increases the interconnected flow path or permeability. In

term of viscosity, the vibration leads to reduce in viscosity as the stability is disturbed by agitation.

Sample	k (md)				Amplitude (mV)		
	Initial	Vib. 1	Vib. 2	Vib. 3	A1	A2	A3
S	6.533	11.027	12.076	12.365	50	5	20
A4	1.036	7.228	5.899	160.772	5	20	50
L	1.619	1.738	1.902	2.616	50	5	20
3	0.24	0.361	0.496	8.214	5	20	50
A6	1.503	7.906	5.039	8.677	5	20	50
1	58.85	0.423	0.203	0.208	5	20	50

Table 2.1: Permeability at different frequencies and amplitudes. (Christian & Tutuka, 2009)

Sample	Dewatering Period (days)				Amplitude (mV)		
	Initial	Vib. 1	Vib. 2	Vib. 3	A1	A2	A3
S	4	2	2	2	50	5	20
A4	11	3	4	1	5	20	50
L	7	7	7	6	50	5	20
3	33	26	19	4	5	20	50
A6	9	3	4	3	5	20	50
1	1.6	21	35	35	5	20	50

Table 2.2: Dewatering period at different frequencies and amplitudes. (Christian & Tutuka, 2009)

The oil extraction from sand for conventional reservoir and methane desorption from inner coal surface are similar in term of vibration stimulation. The experiment was conducted by applying low frequencies and observed the effect of vibration found that the oil extraction rate increases as increases in frequency. When applied frequency is same with the natural frequency of sand which is 25 Hz the wettability changes and reduces the adhesion strength causes the oil extracts from the sand easily. The optimum low frequency range in laboratory scale is also similar in unconventional reservoir at 15-20 Hz yields the better oil extraction efficiency 8.08% comparing stimulation with surfactant alone without vibration effect (Jing et al, 2012)

2.5.2 Surfactant stimulation

Laboratory study conducted by Chen et al, (2006) on the effect of inducing formation damage in coalbed methane by fracture fluids. Irreversible damages of matrix swelling or gel fluids are plugged in the cleat cause permeability impairment. To overcome these damages and reduce in permeability, fracture fluids are prepared to test the improvement of formation. These fluids used in experiment are conventional gel fluid, gel fluid with surfactant and viscoelastic to be flown through the core sample which is placed in the core holder under different overburden/confined pressures adjusted and maintained by pressure holding pump. Pressure transducers at both upstream and downstream are to measure the pressure drop across the core sample and flow rate is measured by gas flow meter located at downstream. The result of this study found out that surface properties improve after adding Ordered Mesoporous Carbons (OMC) 854 surfactants to the base fluids, cross-linked gel. Reduce surface tension, contact angle and increase fluid recovery. Cleanup of the residual fracturing fluids efficiently after stimulation especially for surfactant added to cross-linked gel. Viscoelastic fluid reduces the permeability damage, dewatering period and increases methane production.

Zhang (2004) stated that the potential of natural gas hydrate (NGH) relied on various additives; he also found out that the higher concentration of additive the higher the rate of NGH, its storage capacity and decreases the induction time where induction time is the time when gas is introduced during hydrate formation. ICF (2006) mentioned about the properties of Sodium Dodecyl Sulfate (SDS) or other common name is Sodium Lauryl Sulfate (SLS) that using SDS as surfactant affects the wettability of the fluids on the inner coal surface in which the permeability of water or methane or both is improved.

The statement of Zhang (2004) is consistent with the result of experiment of different surfactants on methane hydrate conducted by Ganji et al (2007) that increasing the concentration of SDS from 300 ppm, 500 ppm to 1000 ppm will boost the disassociation rate of methane hydrate as long as it is below the ice point. As can be seen in figure 2.7 that the optimum concentration of SDS is 500 ppm where the hydrate formation becomes constant at about one hour and higher methane hydrate formation rate comparing to 300 and 1000 ppm. In the same year, they also

conducted experiment of mixed compounds on methane hydrate as well and found out that increasing the rate of surfactant not only increases the methane hydrate but it also boosts the decomposition rate.

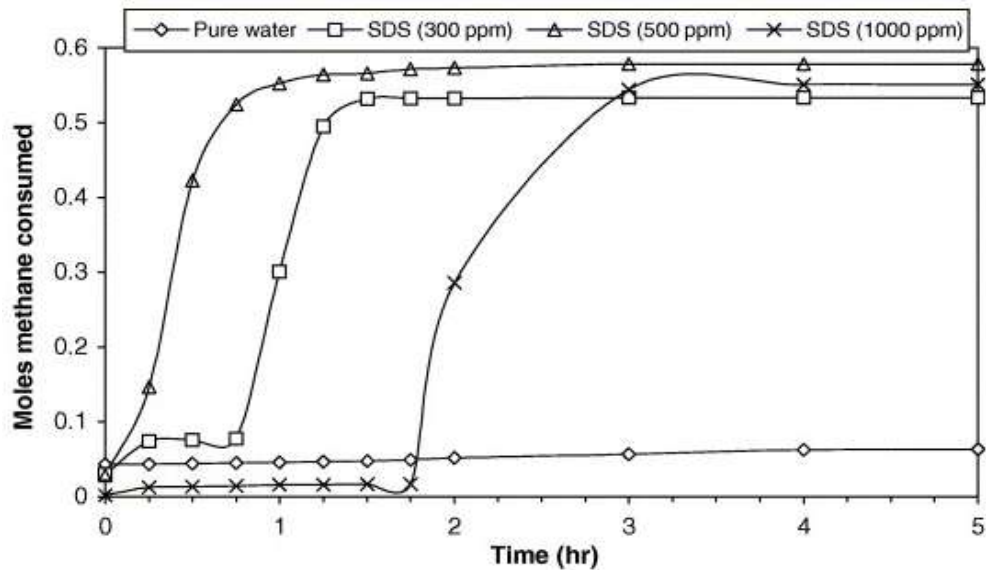


Figure 2.5: Methane hydrate formation rate without SDS and different SDS concentrations in 4.17 mol water (Zhang, 2004)

2.5.3 Temperature stimulation

Laboratory experiment conducted by Zhao, Zhao and Feng (2011) to see the desorption capacity of coalbed methane when affected by the water injection and temperature. Experiment was conducted by increasing temperatures from 15, 20, 25, 30, 35 to 40 degree Celsius. The results of this study found that increasing temperature gives the positive impact on the higher coal rank because it reduces the matrix shrinkage during methane production, increases permeability and coalbed methane recovery ratio. More CBM production increases intensively lead to reduction in temperature downhole and the less permeability in higher coal rank, all these conditions hinder the methane desorption. CBM is put forward to the rising-temperature concept for improving methane desorption as the temperature is more positively correlated with the desorption rather than adsorption. In the same year, Salmachi & Haghghi (2012) also conducted experiment to investigate the effects of temperature on gas sorption. The result of this study is that the methane adsorption affinity reduces 50% with increasing temperatures from 308-348 Kelvin.

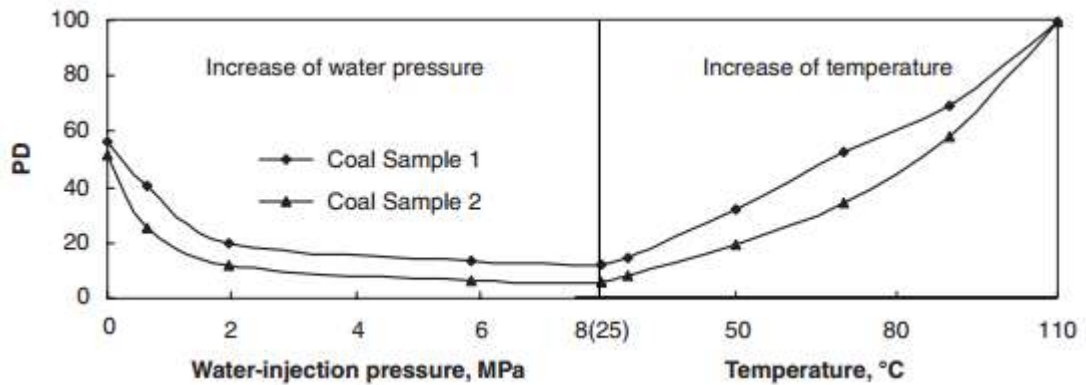


Figure 2.6: The Percentage desorption (PD) as a function of water pressure at constant temperature 25 degree Celsius (left) and function of water temperature at constant 8.0 MPa (right) (Zhao, Zhao and Feng (2011))

As shown in figure 2.6, The PD is the ratio of desorption volume to the adsorption volume. Applying water jet or high water pressure to the coal sample improves the drainage area but prevents the methane from coal thus desorption is low and as temperature increases desorption improves significantly therefore heated hydro-fracture is suitable and feasible for CBM production (Zhao, Zhao and Feng (2011)).

Based on the work of Arenas & Chejne (2004), studied on the effect of temperature and activating agent on porosity. Samples were prepared to undergo different activating agents; carbon dioxide and nitrogen, and different temperatures. The result of this study found out that both activating agent and temperature significantly affect on porosity development. Surface area of coal sample reached maximum at 50% burn-off as the pore wall started to merge due to thermal annealing effect and then decreased at higher temperatures same goes to pore size distribution (PSD) initially increased to maximum and reduced at higher burn-off. Coal rank is also significant parameter influencing the porosity. Coal structure tends to be more compact, microporous structure and less reactive at higher coal rank.

CHAPTER 3

METHODOLOGY

Methodology of this project involves the experiment using frequency, temperature and surfactant in laboratory.

3.1 Correlation between methods and objectives

To make sure the experiment runs smoothly and safely, understand the procedures and awareness of the hazard are important to avoid undesired consequences

Table 3.1: Correlation between the objectives and methodology

Objectives	Methodology
To study the effect of vibration on Malaysian coal samples at specified temperatures	1. Vibration shaker equipment 2. Mercury Porosimeter equipment
To study the effect of surfactant on Malaysian coal samples at specified temperatures	1. Sodium Lauryl Sulfate experiment 2. Mercury Porosimeter equipment

3.2 Materials

1. Malaysian sub-bituminous coal
2. 20 mg Sodium Lauryl Sulfate (SLS) Surfactant in 20 ml water

3.3 Experimental apparatus

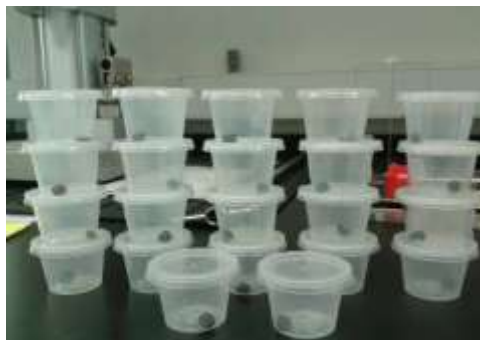


Figure 3.1: Containers



Figure 3.2: Zip lock bags & Al foils



Figure 3.3: Hammer & Cutting tools



Figure 3.4: Density test set



Figure 3.5: Mercury Porosimeter



Figure 3.6: Beakers



Figure 3.7: Vibration Shaker setup



Figure 3.8: Oven

3.4 Control – constraints – constants

Table 3.2: Control, constraints and constants in experiment

Control	Constraints	Constants
Shockproof : Soft papers	Availability of equipment: time gap	Duration of surfactant and temperatures is two hours
Maintain temperature: Aluminium foil, Plastic lock zip and closed container	Uncontinuity	Duration of vibration: one minute and Gravitational force 9.81 m/s^2
One system: Fix the sample on the plate of vibration shaker rigidly by double- sided tape	Fresh samples only: Sample after Mercury Porosimeter cannot be reused due to toxic	20 mg Sodium Lauryl Sulfate in 20 ml water
	Coal samples are very brittle	Initial weight 0.20 grams & density 1.333 g/cm^3

3.5 Experimental procedures / project activities

3.5.1 Coal samples preparation

1. Coal samples were taken from Balingian coalfield, Sarawak Malaysia.
2. The coals were broken into small pieces.
3. Thirteen (13) pieces of 0.2 grams of samples were prepared
4. The density of coal samples were determined as figure 3.4.
 - (i) The sample was weighted in air (gram) by using weighing scale.
 - (ii) The sample was weighted in water (gram) by using density test set. As shown in figure 3.9.
 - (iii) Density (g/cm^3) was calculated from the division of weight in air over the difference between the weight in air and weight in water.
5. The samples were dried in the oven at $100 \text{ }^\circ\text{C}$ for two hours.

6. The properties of coal sample was measured by using Mercury Porosimeter (figure 3.5). Noted that weight in air and density are required prior performing the measurement.

7. The prepared samples were wrapped by Aluminium foil, kept in closed container and plastic zip lock for next experiments.



Figure: 3.9: Density test setup

3.5.2 Effect of temperatures

1. Four (4) coal samples were prepared.
2. Each sample was dried in the oven at 30, 50, 70 and 90 °C for two hours.
3. The density of coal samples were determined as figure 3.4.

(i) The sample was weighted in air (gram) by using weighing scale.

(ii) The sample was weighted in water (gram) by using density test set. As shown in figure 3.9.

(iii) Density (g/cm^3) was calculated from the division of weight in air over the difference between the weight in air and weight in water.

4. The density tested sample was dried in the oven at 100 °C for two hours.
5. The properties of coal sample was measured by using Mercury Porosimeter (figure 3.5). Noted that weight in air and density are required prior performing the measurement.

3.5.3 Effect of surfactant stimulation

1. Two coal samples were prepared
2. One coal sample was dried in the oven at 50 °C for two hours and another one at 70°C for two hours and wrapped by Aluminium foil, kept in closed container and plastic zip lock for next experiments as shown in figure 3.10.



Figure 3.10: Maintain the temperature of the coal samples

3. Both coal samples were dip in 20 mg Sodium Lauryl Sulfate surfactant dissolved in 20 ml water for two hours as figure 3.11.



Figure 3.11: Dipping sample in the Sodium Lauryl Sulfate surfactant

4. The tested samples were dried in the oven at 100 °C for two hours.
5. The density of coal samples were determined as figure 3.4.
 - (i) The sample was weighted in air (gram) by using weighing scale.
 - (ii) The sample was weighted in water (gram) by using density test set. As shown in figure 3.9.
 - (iii) Density (g /cm^3) was calculated from the division of weight in air over the difference between the weight in air and weight in water.
6. The density tested samples were dried in the oven at 100 °C for two hours.
7. The properties of coal sample was measured by using Mercury Porosimeter as shown in figure 3.5. Noted that weight in air and density are required prior performing the measurement.

3.5.4 Effect of vibration stimulation

1. Six (6) coal samples were prepared
2. Three (3) coal samples were dried in the oven at 50 °C for two hours and three coal samples at 70°C for two hours as figure 3.10.
3. The coal sample was stuck on the plate of the vibration shaker, as figure 3.12.
4. The vibration shaker was connected to the electronic controller.

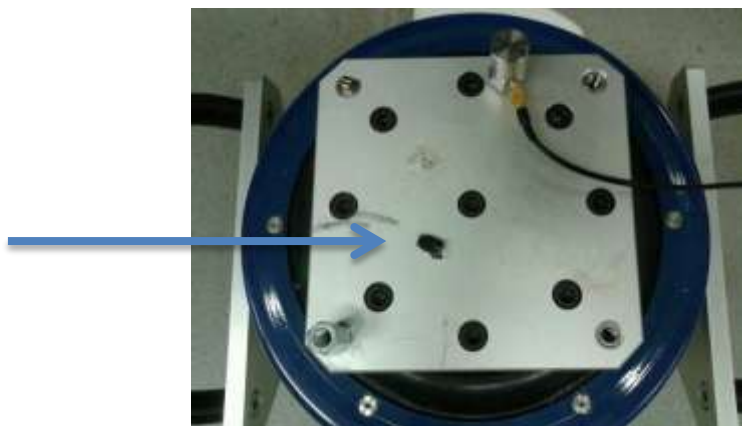


Figure 3.12: The coal sample was stuck on the plate of vibration shaker

5. Frequencies were applied at 50 Hz, 100 Hz and 200 Hz for one minute. Each frequency was applied on two coal samples at 50°C and 70°C.

6. The density of coal samples were determined as figure 3.4.

(i) The sample was weighted in air (gram) by using weighing scale.

(ii) The sample was weighted in water (gram) by using density test set. As shown in figure 3.9.

(iii) Density (g/cm^3) was calculated from the division of weight in air over the difference between the weight in air and weight in water.

7. The properties of coal sample was measured by using Mercury Porosimeter (figure 3.5). Noted that weight in air and density are required prior performing the measurement.

3.6 Research methodology

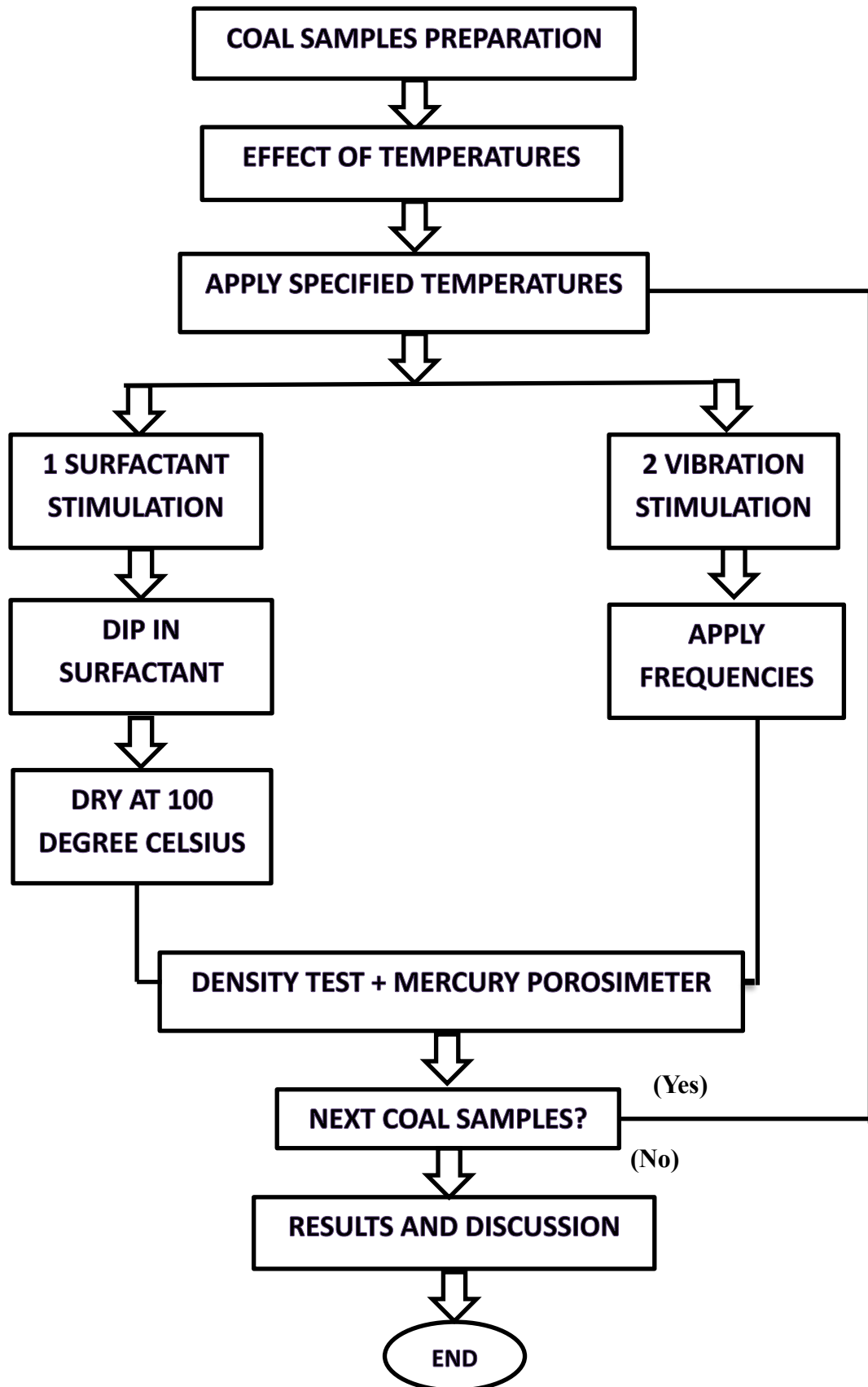


Figure 3.13: Research methodology

3.7 Key milestones

3.7.1 Final Year Project 1

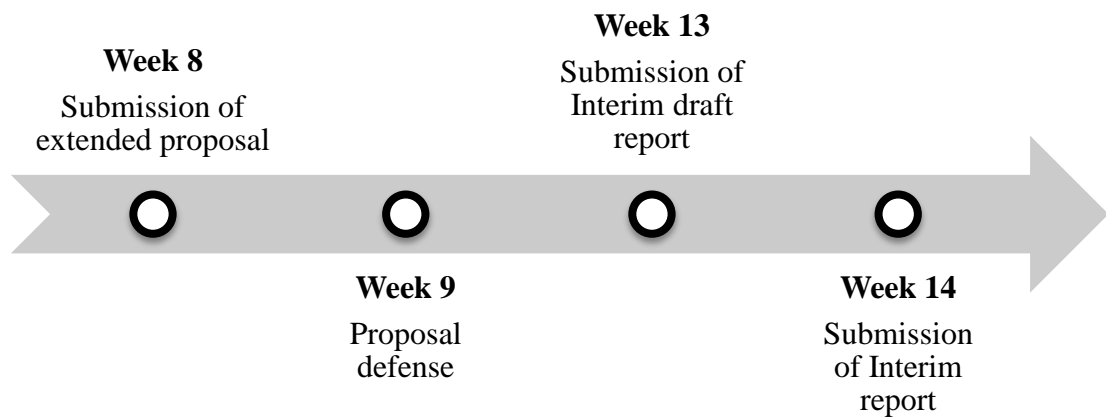


Figure 3.14: Project key milestone for FYP1

3.7.2 Final Year Project 2

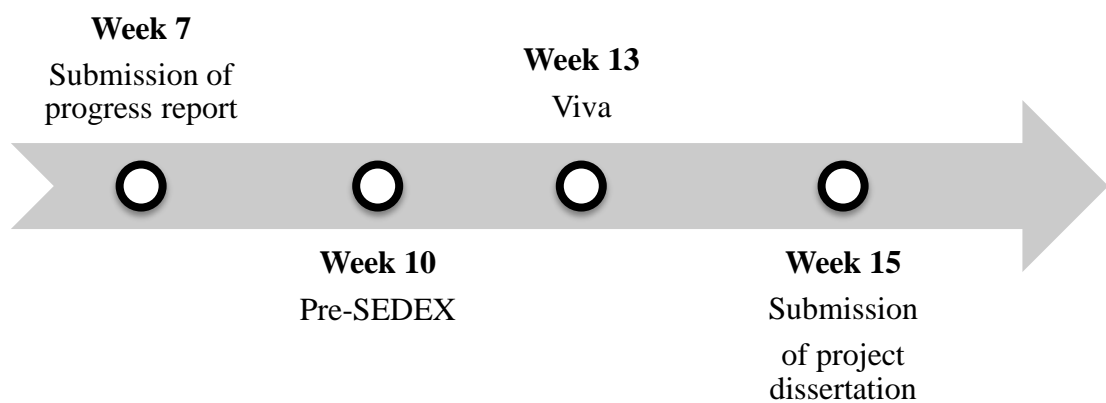


Figure 3.15: Project key milestone for FYP2

3.7.3 Experiments Key Milestones

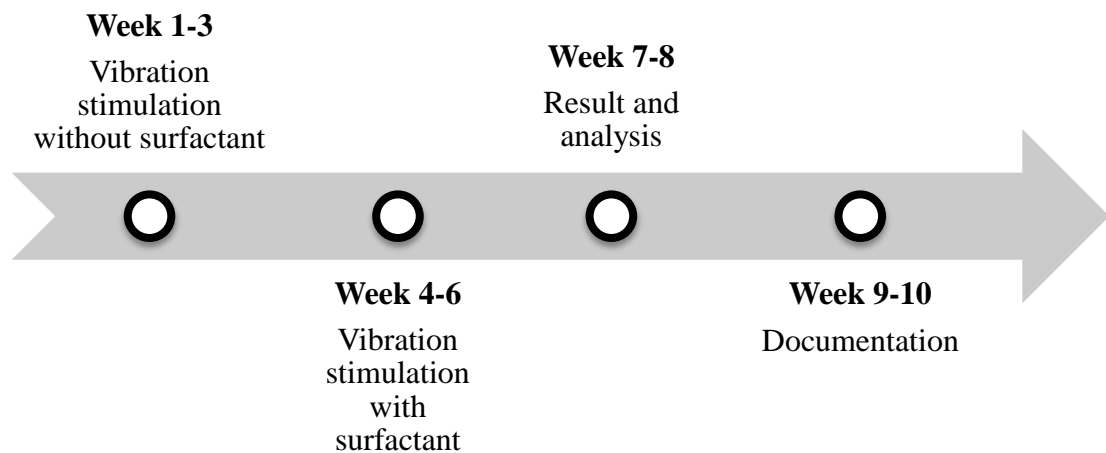


Figure 3.16: Experiments Key Milestones for FYP2

3.8 Gantt chart

3.8.1 Final year project 1

No	Detail/ Week	1	2	3	4	5	6	7	8	9	10	11	12	13	14
1	Confirmation of project topic and supervisor	■	■												
2	Preliminary Research work		■	■	■	■	■	■							
3	Submission of Extended proposal								■						
4	Proposal Defense									■					
5	Project work continue										■	■	■		
6	Submission of Interim draft report													■	
7	Submission of Interim report														■

Table 3.3: Gantt chart for Final Year Project 1

3.8.2 Final year project 2

No	Detail/ Week	1	2	3	4	5	6	7	8	9	10	11	12	13	14	15
1	Project work continues	■	■	■	■	■	■	■								
2	Submission of Progress Report							■								
3	Project work continues								■	■	■	■	■			
4	Pre-Sedex										■					
5	Submission of Draft final report											■				
6	Submission of dissertation (soft bound)												■			
7	Submission of Technical Paper												■			
8	Viva													■		
9	Submission of Project Dissertation (Hard bound)															■

Table 3.4: Gantt chart for Final Year Project 2

3.8.3 Overall experiments against gantt chart

No	Detail/ Week	1	2	3	4	5	6	7	8	9	10	11	12	13	14	15
1	Supervisors Consultation															
2	Stimulation design planning															
3	Booking the equipment															
4	Coal samples preparation															
5	Density test															
6	Temperature stimulation															
7	Surfactant stimulation															
8	Mercury Porosimeter Measurement															
9	Documentation															
10	Vibration stimulation															

Table 3.5: Gantt chart of overall experiments for Final Year Project 2

CHAPTER 4

RESULTS AND DISCUSSION

Coal samples were prepared and undergone under different stimulation methods which are temperature, vibration and surfactant. The following sections describe the effect of change on coal characteristics after stimulation methods.

4.1 Effect of temperatures on coal

Table 4.1: Coal properties after effect of temperatures

Sample	Porosity (%) Base case	Permeability (md) Base case	Temperature (°C)	Porosity (%)	Total specific volume (mm^3/g)	Specific pore surface area (m^2/g)
S_A	-4.93	0.475	30	14.93	97.26	13.897
S_O			50	11.61	68.95	16.709
S_B			70	12.02	74.09	13.704
S_C			90	-6.33	-29.45	-6.654

Based on Figure 4.1, Applying temperatures range from 30,50,70 and 90°C found out that temperature significantly affect the total specific volume of coal which is the total volume per unit mass of coal. The trend for porosity and total surface are relatively the same. However optimum porosity , specific volume and total surface area are at 30 degree Celsius where porosity and specific volume yield highest. Based on the research of Arenas & Chejne (2004) mentioned that 20% of burn off, merging of pores are dominant and decreasing in surface areas after high burn-off due to the conversion of micropore into meso- and macropores. This experiment is consistent with his work on the development of surface area that maximum surface area is reached at 50% burn off and gradually decreased. Same goes to PSD that will decrease at higher burn off. Noted that data from table 4.1 refer to Appendices

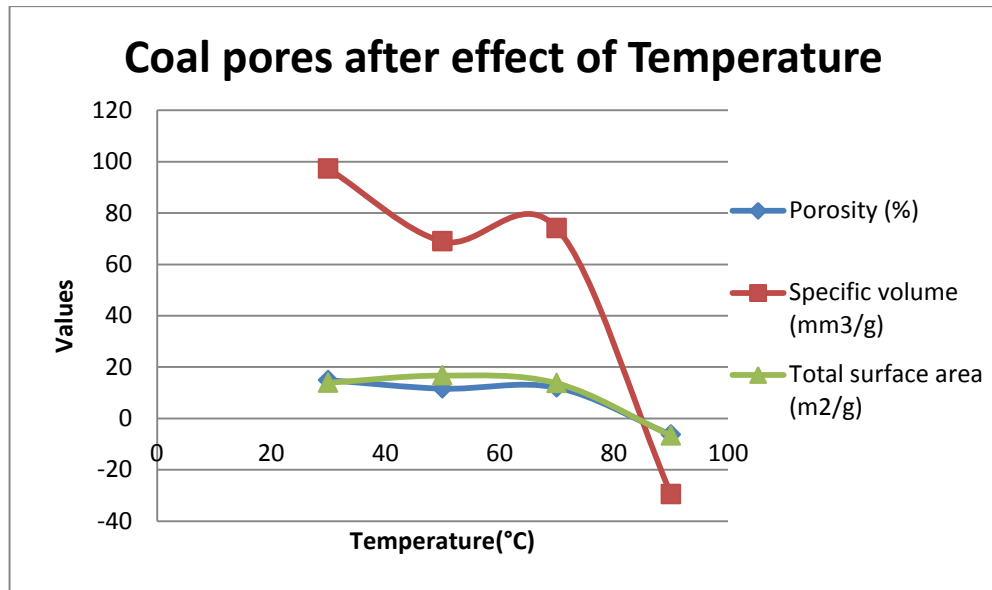


Figure 4.1: Coal pores curves after effect of temperatures

4.2 Effect of temperatures on porosity & permeability

Table 4.2: Porosity&Permeability results after effect of temperatures

Sample	Temperature (°C)	Tortuosity (μm ²)	Permeability (md)	Porosity (%)
<i>S_A</i>	30	354.74x 10 ⁻⁶	0.359	14.93
<i>S_O</i>	50	942.43x 10 ⁻⁷	0.095	11.61
<i>S_B</i>	70	167.82x 10 ⁻⁶	0.170	12.02
<i>S_C</i>	90	167.82x10 ⁻⁶	0.170	-6.33

Noted that since only tortuosity is provided in Mercury porosimeter report to determine the permeability of the coal sample, here is the steps how to obtain permeability from tortuosity and these steps will be applied throughout the report.

Based on International system of units (SI) stated the conversion of one square meter to darcy as following;

$$1 \text{ m}^2 = 1.013249966 \times 10^{12} \text{ D and } 1 \text{ } \mu\text{m}^2 = 10^{-12} \text{ m}^2 = 1.013249966 \text{ D}$$

Thus **Permeability (mD) = Tortuosity (μm²) x 1.013249966 D**

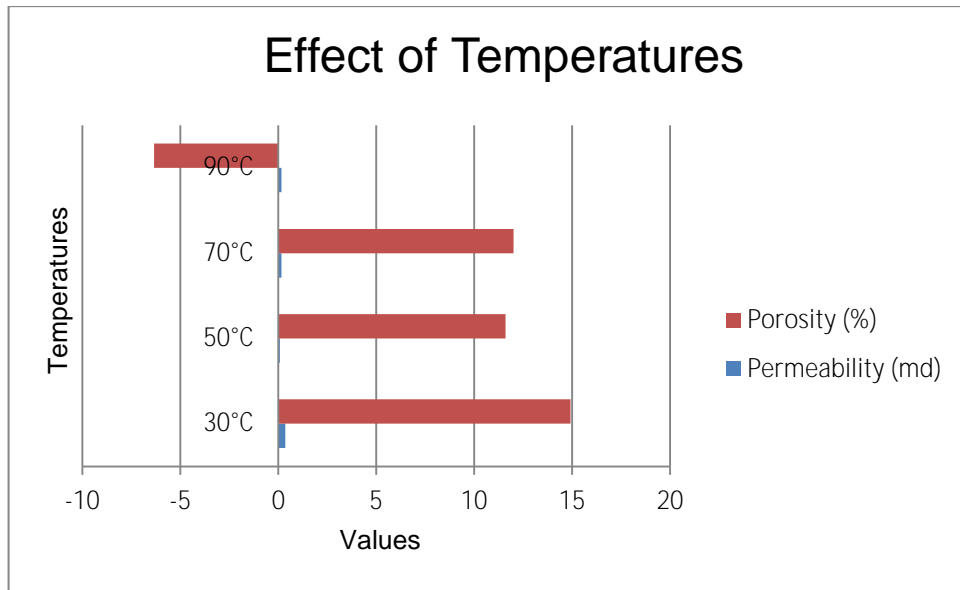


Figure 4.2: Porosity & permeability bar charts after effect of temperatures

Based on Table 4.2 and Figure 4.2, temperature predominantly affects the porosity rather than permeability. The development of porosity and permeability as a function of temperature: porosity and permeability increased to a maximum value at optimum temperature 30°C and then decreased. These developments depend, in unpredictable ways on different factors encountered. The highest porosity and permeability are reached at 30°C due to thermal annealing phenomenon that is the reduced porosity at higher temperatures and the higher the rank coal, the samples tend to be less reactive coal lead to more microporous structure. These results are consistent to the work of Arenas & Chejne (2004). Noted that data from table 4.2 refer to Appendices

4.3 Effect of surfactant stimulation on coal

Table 4.3: Coal pores properties after effect of surfactant stimulation

Sample	Temperature (°C)	Porosity (%)	Total specific volume (cc/g)	Specific pore surface area (m ² /g)
5 ₅	50	2.05	16.21	-12.682
5 ₆	70	3.79	34.69	2.109

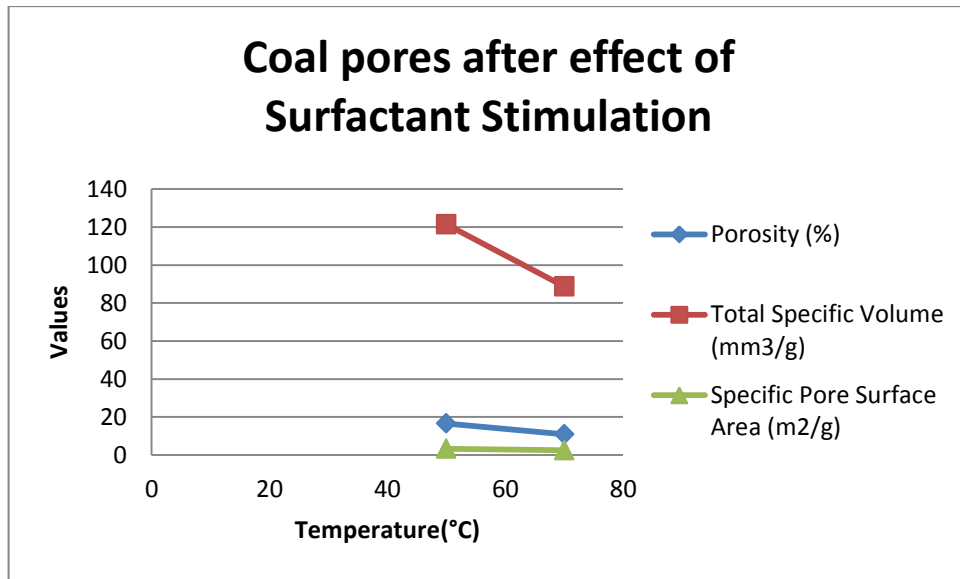


Figure 4.3: Coal pores curves after effect of surfactant stimulation

Based on table 4.3 and figure 4.3, 20 ml Sodium Lauryl Sulfate (SLS) Surfactant in 20 ml water was applied. The results found out that at constant concentration of surfactant, the porosity, total specific volume and specific pore surface increase at higher temperature from 50 to 70 °C. the porosity and surface area are relatively low. Based on the work of Ganji et al (2007) found out that increasing surfactant SLS concentration will increase the methane hydrate which is preferable in desorption of methane. It can be concluded that increasing temperature and concentration at optimum will yield the desired result for CBM stimulation. Noted that data from table 4.3 refer to the appendices.

4.4 Effect of surfactant stimulation on porosity&permeability

Table 4.4: Porosity&permeability results after effect of surfactant stimulation

Sample	Temperatures (°C)	Tortuosity (μm^2)	Permeability (md)	Porosity (%)
S_1	50	337.93×10^{-4}	0.034	2.05
S_2	70	469.25×10^{-6}	0.475	3.79

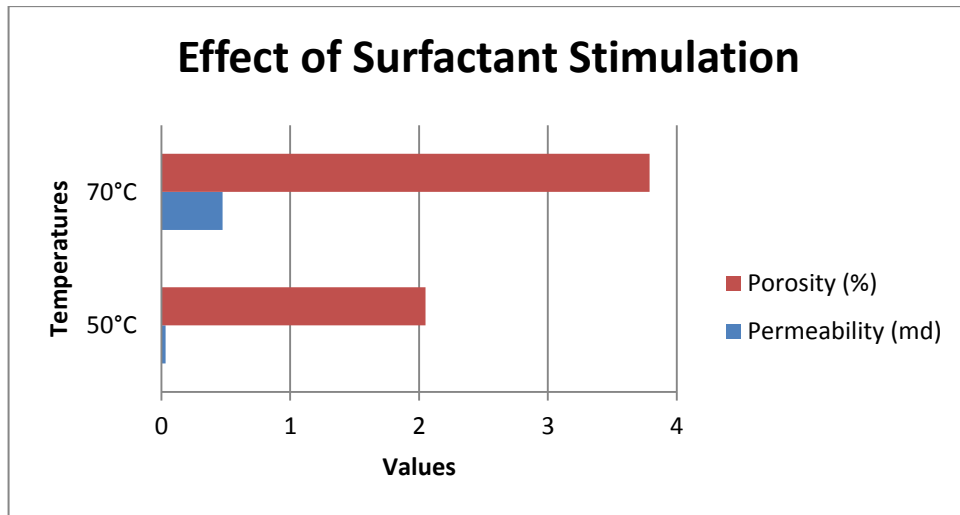


Figure 4.4: Porosity&permeability bar charts after effect of surfactant stimulation

Based on Table 4.4 and figure 4.4, Surfactant stimulation where concentration and volume are fixed constant throughout. The results found out that surfactant significantly affect the porosity and permeability of the coal samples. Increasing temperatures, coal characteristics trends tend to increase eventhough the ranges are quite small. In general, Increase the volume and concentration the porosity and permeability will also increase. It is believed that the surfactant helps to reduce the surface tension, contact angle and increase fluid recovery. Data from table 4.4 refer to the appendices.

4.5 Effect of vibration stimulation on coal

Table 4.5: Coal pores properties after effect of vibration stimulation

Temperature (°C)	Sample	Frequency (Hz)	Porosity (%)	Total specific volume (mm^3/g)	Specific surface area (m^2/g)
50	S_3	50	16.59	121.43	3.295
	S_4	100	N/A		
	S_5	200	10.91	88.77	2.527
70	S_6	50	17.55	127.66	16.105
	S_7	100	-2.23	-15.61	-12.845
	S_8	200	2.57	23.08	-2.536

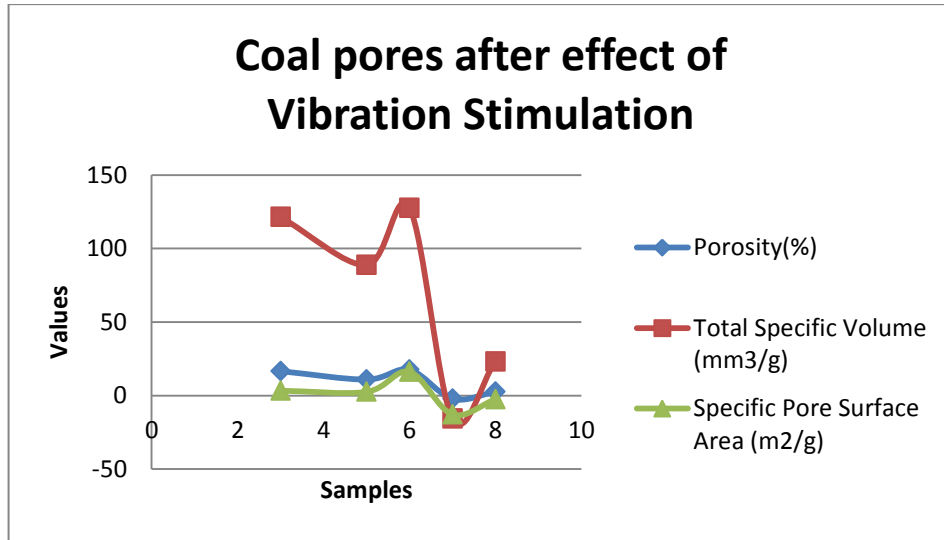


Figure 4.5: Coal pores curves after effect of vibration stimulation

Based on table and figure 4.5, Vibration stimulation is applied by using vibration shaker. The results found out that at sample of 50°C Sample 3 and 5, increasing frequency will yield the lower porosity, specific volume and surface area while for sample of 70°C which are sample 6,7 and 8 yield the optimum at 50 Hz then gradually decrease and increase at 200Hz. The negative values indicate the deformation of internal structure that deteriorates the coal pores. For sample at 50°C and 100 Hz is not available due to technical problem occurred during measurement using mercury porosimeter, this constraint refers to table 3.2. It can be concluded that the optimum frequency of both temperature at 50°C and 70°C are at 50 Hz with relatively high value of porosity which is the desired effect of CBM stimulation.

4.6 Effect of vibration stimulation on porosity & permeability

Table 4.6: Porosity&permeability results after effect of vibration stimulation

Temperature (°C)	Sample	Frequency (Hz)	Tortuosity (μm^2)	Permeability (md)	Porosity (%)
50	S_3	50	110.28×10^{-4}	11.2	16.59
	S_4	100	N/A		
	S_5	200	639.45×10^{-5}	6.479	10.91
70	S_6	50	542.68×10^{-6}	0.549	17.55
	S_7	100	542.68×10^{-6}	0.549	-2.23
	S_8	200	542.68×10^{-6}	0.549	2.57

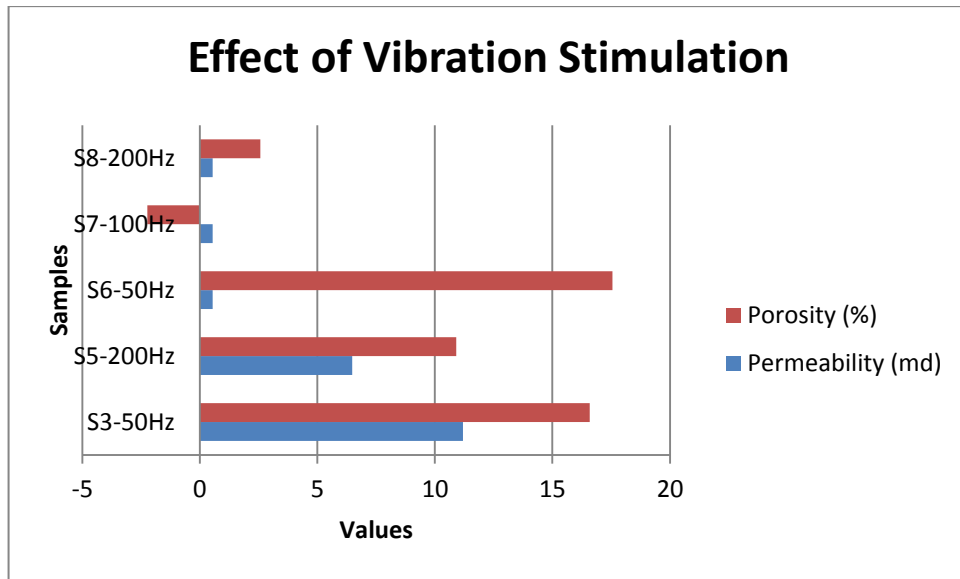


Figure 4.6: Porosity&permeability bar charts after effect of vibration stimulation

According to table 4.6 and table 4.6 found out that maximum porosity for both samples at 50°C and 70°C (S3&S6) are at optimum 50 Hz and tends to reduce after optimum frequency. For sample at 70°C (S7), at 100 Hz, porosity is severely low and gradually increases at 200 Hz, In addition, maximum permeability of the sample at 50°C is at optimum 50 Hz (S3) and gradually decrease while the permeabilities of sample at 70 °C (S6,S7&S8) remain thoroughly constant at 0.549 mD at 50, 100 and 200 Hz therefore frequency does not significantly affect the sample at 70 °C. noted that density after effect of vibration stimulation is reduced. Ariadji (2005) described the mechanism of vibration that the agitation due to vibration helps to connect the non-connective porosity, reduce the surface tension, reduce the tortuosity thus increase the interconnected flow path or permeability. Noted that data from table 4.5 and 4.6 refer to the appendices.

4.7 Sample compressibility

Table 4.7: Compressibility results after stimulation effects

Stimulation method	Sample	Sample compressibility (1/MPa)	Permeability (md)
Effect of temperatures	S_A at 30°C	1.144×10^{-3}	0.359
	S_O at 50°C	2.336×10^{-3}	0.095
	S_B at 70 °C	1.532×10^{-3}	0.170
	S_C at 90°C	7.197×10^{-3}	0.170
Effect of surfactant	S_1	4.034×10^{-3}	0.034
	S_2	4.009×10^{-3}	0.475
Effect of vibration	S_3 at 50 Hz	1.784×10^{-5}	11.2
	S_5 at 200 Hz	0.000	6.479
	S_6 at 50 Hz	0.000	0.549
	S_7 at 100 Hz	6.353×10^{-3}	0.549
	S_8 at 200 Hz	2.810×10^{-3}	0.549

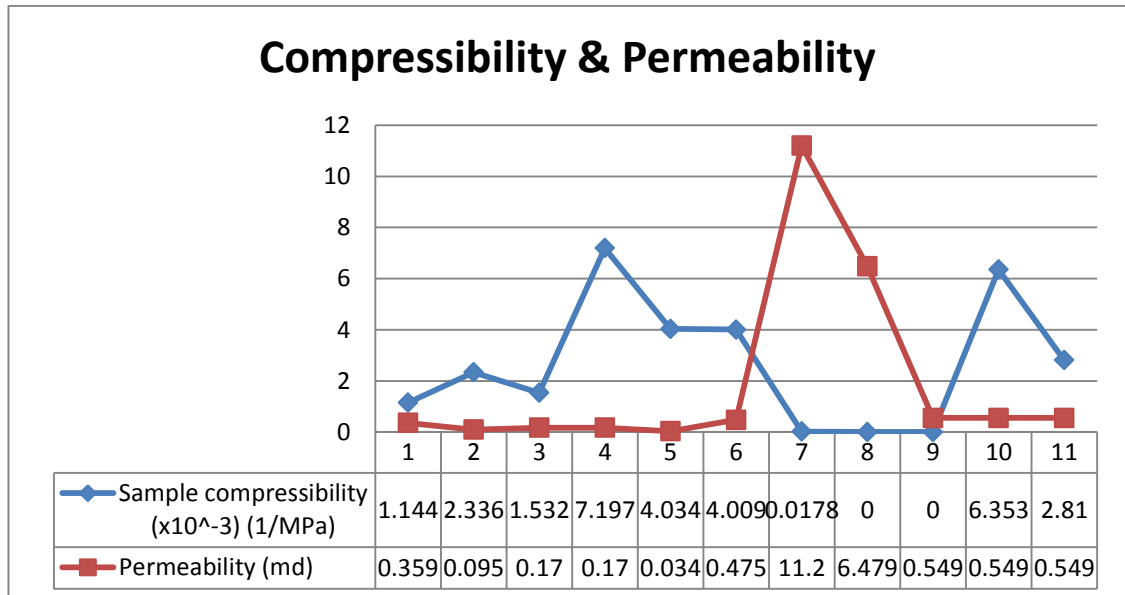


Figure 4.7: Compressibility and permeability curves after stimulations

According to Compressibility and Permeability curves after effect of stimulations. On the x-axis 1 to 4 are effect after temperature, 5 to 6 are effect after surfactant

stimulation and 7 to 11 are effect after vibration stimulation. The results found out that the lower the sample compressibility the higher permeability. Apparently reached the peak during vibration stimulation effect at point 7 which is vibration at 50 Hz and 50°C and gradually decreases at higher frequency (100 Hz and 200 Hz) and also for higher temperature of sample 70°C at 50 Hz, 100 Hz and 200 Hz. Effect of temperatures, permeabilities are relatively low due to increase in sample compressibility whereas surfactant stimulation effect is not dominant. It can be concluded that effect of vibration stimulation yields the relatively high permeability at low compressibility. When frequency is applied, increase in stress, the coal tends to gradually bend or **build** the rock until it exceeds the internal strength changes its internal structure and cause fractures. In general, increase in stress will decline the compressibility. Harpalani & Schraufnagel (1990) stated that proper sample compressibility is important parameter and necessary for analyzing long-term production data or during drawdown. Noted that data from table 4.7 refer to the appendices.

4.8 Density calculations

Table 4.8: Results of density measurement experiment

Sample	Type of stimulations	Weight in air (g)	Weight in water (g)	Density (g/cm ³)
S_{Base}	Without stimulations	0.20	0.05	1.333
S_A at 30°C	Temperatures	0.20	0.05	1.333
S_O at 50°C		0.20	0.05	1.333
S_B at 70 °C		0.20	0.05	1.333
S_C at 90°C		0.20	0.05	1.333
S_1	Surfactant	0.18	0.04	1.286
S_2		0.18	0.04	1.286
S_3 at 50 Hz	Vibration	0.18	0.04	1.286
S_4 at 100 Hz		0.18	0.04	1.286
S_5 at 200 Hz		0.18	0.04	1.286
S_6 at 50 Hz		0.18	0.04	1.286
S_7 at 100 Hz		0.18	0.04	1.286
S_8 at 200 Hz		0.18	0.04	1.286

$$\text{Density(g/cm}^3\text{)} = \frac{[A]}{[A] - [B]}$$

[A]: Weight in air (g)

[B]: Weight in water (g)

Density and weight in air of samples are needed for Mercury porosimeter equipment. The initial weight of sample is 0.20 grams. Based on table 4.8, found out that the effect after temperatures, Density and initial weight remain constant whereas surfactant and vibration stimulation slightly affect on density values but it indicates that after stimulations, the internal structure of the samples do change

CHAPTER 5

CONCLUSION AND RECOMMENDATIONS

Conclusion after thorough literature review, it can be concluded that the effect of change in coal characteristics were observed after surfactant and vibration stimulation at specified temperatures. Based on literatures and experiment, the conclusion of this study are

- At 30°C which is the optimum temperature after effect of temperatures yields better improvement of coal characteristics.
- Surfactant stimulation yields the desired effect of CBM stimulation at higher temperature and concentration.
- Optimum frequency for both 50°C and 70°C are at 50 Hz significantly yields the high value of porosity and permeability which are the positive effect on coal characteristic after vibration stimulation.
- Sample compressibility and permeability are **inversely proportion** to one another. Compressibility from this experiment can help to provide the proper compressibility for long term production analysis.

Recommendation on future studies on the effect of desorption and coal characteristics at constant temperature under different pressures can be conducted with the same procedures and modified current setup. In addition for future recommended on this project is to conduct experiments with wider ranges of temperatures and different types of wave for example acoustic waves, electromagnetic waves at different frequencies and also apply different volumes of Sodium Lauryl Sulfate surfactant or different types of surfactant for broader and comprehensive results. It is highly preferable to invent the integral equipment where it contains the installed vibration generator, temperature regulator and injection path of fluid into one whole equipment to avoid such errors from environment and so on.

Objectives were achieved with the successful outcome of Coalbed methane stimulations by using surfactant and frequencies. The results of this project will be helpful in finding the suitable method for CBM stimulations and hopefully this project can bring some new changes on CBM study.

REFERENCES

- Anderson, J., 2003. Producing Natural Gas From Coal, *Oilfield Review*, Autumn.
- Arenas, E., & Chejne, F. (2004). The effect of the activating agent and temperature on the porosity development of physically activated coal chars. *CARBON*, 42(12), 2451-2455.
- Ariadji, T., 2005. Effect Of Vibration On Rock And Fluid Properties: On Seeking the Vibroseismic Technology Mechanisms, SPE 93112 presented at the 2005 Asia Pacific Oil & Gas Conference and Exhibition.
- Bhattacharya, S.K., & Tunio, S. Q.. (2013). "CBM a Pathfinder of Petroleum System" *Research Journal of Applied Sciences, Engineering and Technology*, 7(13), 2622-2626.
- Chen, Z., Khaja, N., Valencia, K., & Rahman, S. S. (2006, January 1). Formation Damage Induced by Fracture Fluids in Coalbed Methane Reservoirs. Society of Petroleum Engineers.
- Christian, T., and Tutuka, A., 2009. Seeking effects of vibration stimulation on coalbed methane (CBM) reservoir to accelerate gas production using laboratory and reservoir stimulation studies.
- Ganji, H., Manteghian, M., Sadaghiani Zadeh K., Omidkhah, M.R., Rahimi Mofrad, M.R.. (2007). Effect of different surfactants on methane hydrate formation rate, stability and storage capacity, *Fuel* 86, 434–441.
- Ganji, H., Manteghian, M., Mofrad, H.R. (2007). Effect of mixed compounds on methane hydrate formation and dissociation rates and storage capacity, *Fuel Processing Technology*, 88, 891–895.
- Grattoni, C. A., Ahsan, M., Durucan, S., & Jing, X. D. (2006). Measurements of petrophysical properties of coal for CO₂ sequestration

- Harpalani, S., & Schraufnagel, R. A. (1990). Influence of Matrix Shrinkage and Compressibility on Gas Production From Coalbed Methane Reservoirs; Society of Petroleum Engineers.
- Kong, C. C., Irawan, S., Chow, W. S., & Tunio, S. Q. (2011). "Preliminary study on gas storage capacity and gas-in-place for cbm potential in balingian coalfield, sarawak malaysia". *International Journal of Applied Science and Technology*, 82-94.
- Lin, W. (2010), "Gas Sorption and the Consequent Volumetric and Permeability Change of Coal", Department of Resource Engineering, Stanford University.
- Miller B. G. (2005), "Coal Energy Systems". Elsevier Academic Press (pp. 1, 2, 6)
- Mohamed, A.R. & Lee, K.T., 2004. "Energy Policy for Sustainable Development in Malaysia", Paper no. 9-028 (O). Prepared for presentation at The Joint International Conference on Sustainable Energy and Environment (SEE) held in Hua Hin, Thailand, 1-3 December 2004
- Moore, T.A., 2012, "Coalbed Methane: A review," *International Journal of Coal Geology* 101: 36-81. Elsevier
- Ramaswamy, S. (2007). *Selection of best drilling, completion and stimulation methods for coalbed methane reservoirs*. Unpublished master's thesis, Texas A&M University, Texas, United States.
- Rice, D. D., & Claypool, G. E. (1981). Generation, accumulation, and resource potential of biogenic gas. *AAPG Bulletin*, 65(1), 5-2.
- Rightmire, C.T., 1984., Coalbed methane resources, in Rightmire, C.T., Eddy, G.E., and Kirr, J.N., editors, Coalbed methane resources of the United States: American Association of Petroleum Geologists Explorer, v. 21, no.4 (April, 2000), p. 16, 1820, 22-23.
- Roadifer, R.D. and Moore, T.R., 2003 Coalbed Methane Parametric Study: What's Really Important to Production and When?, SPE 84425 presented at the 2003 SPE Annual Technical Conference and Exhibition, Denver.

Rogers, R.E., 1994. *Coalbed Methane: Principles & Practice*, Prentice Hall, England.

Salmachi, A., & Haghghi, M. (2012). Temperature effect on methane sorption and diffusion in coal: application for thermal recovery from coal seam gas reservoirs. *APPEA Journal*, 52:291-300.

Tarek, A., Nathan, D. (2012). *Advanced Reservoir Management and Engineering* (2nd Edition).Elsevier

Tanuwijaya, C., & Ariadji, T. (2009). Seeking Effects of Vibration Stimulation on Coalbed Methane (CBM) Reservoir to Accelerate Gas Production using Laboratory and Reservoir Stimulation Studies. *JTM*, 4.

Trevor, M. (1996). *Genesis and the Origin of Coal and Oil*. Montgomery,AL USA: Apologetics Press, Inc.

Tunio, S. Q., Nair, P., & Irawan, S. (2012). Forecasting CBM Production of Mukah Balingian Coalfield, Sarawak, Malaysia. *Research Journal of Applied Sciences, Engineering and Technology*.

Zhang, C.S., Fan, S.S., Liang, D.Q., Guo, K.H., (2004). Effect of additives on formation of natural gas hydrate. *Fuel* 83, 2115–2121.

Zhao, D., Zhao, Y., & Feng, Z. (2011). Laboratory Experiment on Coalbed-Methane Desorption Influenced by Water Injection and Temperature. *Journal of Canadian Petroleum Technology*(50), 24-33.

Alberta Energy (2013). Coal Maturation and Coalbed Methane Generation. Retrieved as on 29/6/2014 from website
http://www.agr.gov.ab.ca/energy/cbm/coal_and_cbm_intro2.html

Coalbed methane: Principles and practices (2008). Halliburton Inc.

Retrieved as on 29/6/2014 from website

http://www.halliburton.com/public/pe/contents/Books_and_Catalogs/web/CBM/H06263_Chap_01.pdf

ICF (2006). Sodium Lauryl Sulfate, Technical Evaluation Report. Retrieved as on 17/8/2014 from website

<http://www.pharmsolutions.com/docs/NationalOrganicProgramReportonSodiumLaurylSulfate.pdf>

Jing, L., Sheng, C., Sen, X., Ming, L., Wei, G. (2012) . "Experimental study on synergistic effect mechanisms of surfactant assisted by low frequency vibration waves." Retrieved as on 18/8/2014 from website [http://www.thefreelibrary.com/Experimental study on synergistic effect mechanisms of surfactant...-a0323659181](http://www.thefreelibrary.com/Experimental+study+on+synergistic+effect+mechanisms+of+surfactant...-a0323659181)

Schlumberger Glossary. Retrieved as on 29/6/2014 from website <http://www.glossary.oilfield.slb.com/en/Terms.aspx?LookIn=term%20name&filter=CB>

Virginia Energy (n.d). Whence this Coal?. Retrieved as on 1/7/2014 from website <http://virginiaenergy.weebly.com/coal-formation----april-15.html>

APPENDICES

MERCURY POROSIMETER RESULTS

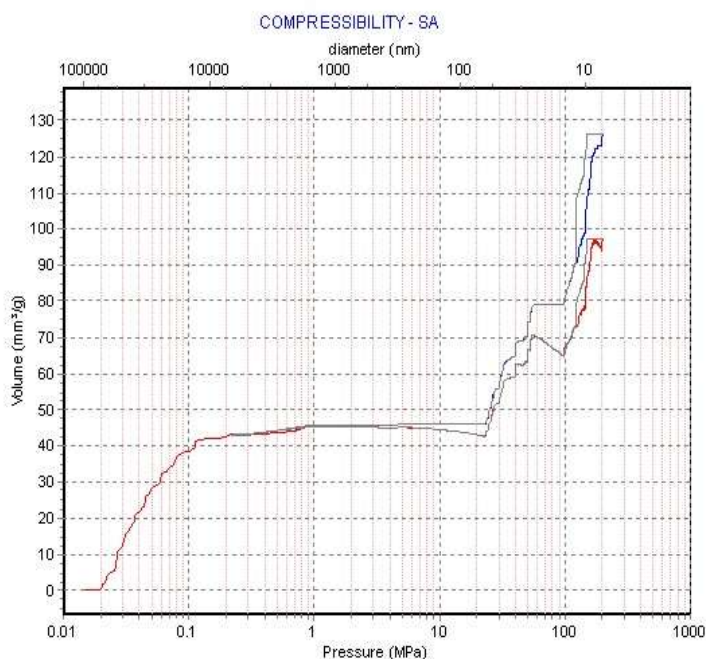
- Sample A

ThermoFisher
SCIENTIFIC

COMPRESSIBILITY CORRECTION

SA
Comment

Report date:14-10-14



RESULTS WITH COMPRESSIBILITY CORRECTION

Correction enabled (Y/N):	Yes
Linearity range:	From (MPa): 160.5690 To (MPa): 200.7112
Correction factor (mm³/g.MPa)	0.144389
Compressibility factor (MPa.g/mm³)	6.9258
Compressed volume (mm³/g):	28.98
Sample compressibility (1/MPa):	1.144E-3
Bulk modulus (MPa):	8.743E+2

Total intruded volume (mm³/g):	97.26 at pressure (MPa): 200.7112
Intruded vol. (mm³):	8.42
Envelope density (g/cm³):	1.5349
Bulk density @ pressure (g/cm³):	1.6409 at pressure (MPa): 0.1735
Apparent density (g/cm³):	1.8043 at pressure (MPa): 200.7112
Real void volume by real dens. (mm³/g):	-98.68
Accessible porosity (%):	14.93
Inaccessible porosity (%):	-30.08

Surface area model:	Cylindrical and Plate
Tortuosity (Carniglia):	2.061

Tortuosity extended calculated:	from Tortuosity
Exponent cylindrical pore:	1.754
Tortuosity extended (Carniglia):	1.638

RESULTS OF PERMEABILITY:

Cylindrical pores permeability (µm²):	365.62E-6
General permeability calculated:	from Tortuosity
General permeability (µm²):	354.74E-6

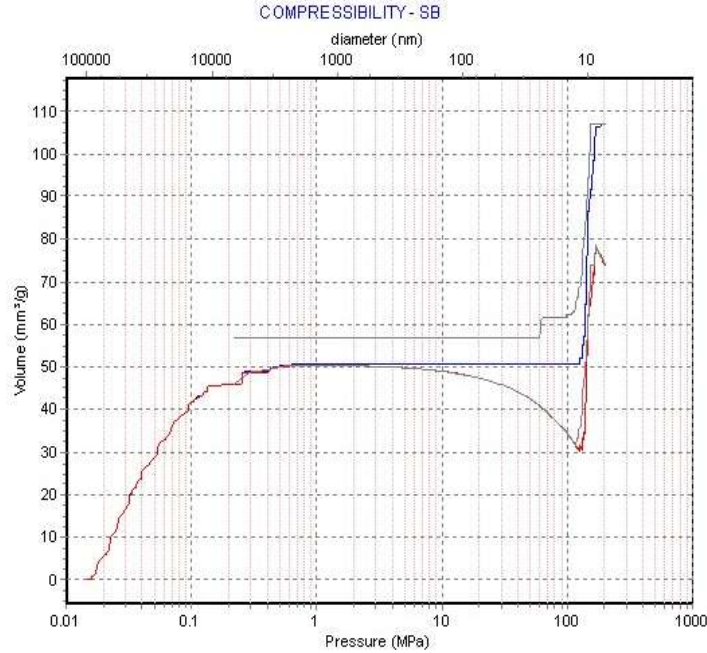
• **Sample B**

ThermoFisher
SCIENTIFIC

SB
Comment

Report date:14-10-14

COMPRESSIBILITY CORRECTION



RESULTS WITH COMPRESSIBILITY CORRECTION

Correction enabled (Y/N):	Yes		
Linearity range:	From (MPa):	160.6489	To (MPa): 200.8111
Correction factor (mm ³ /g.MPa)	0.164008		
Compressibility factor (MPa.g/mm ³)	6.0973		
Compressed volume (mm ³ /g):	32.93		
Sample compressibility (1/MPa):	1.532E-3		
Bulk modulus (MPa):	6.526E+2		
Total intruded volume (mm ³ /g):	74.09 at pressure (MPa):	200.8111	
Intruded vol. (mm ³):	9.13		
Envelope density (g/cm ³):	1.6226		
Bulk density @ pressure (g/cm ³):	1.7525	at pressure (MPa):	0.1735
Apparent density (g/cm ³):	1.8443	at pressure (MPa):	200.8111
Real void volume by real dens. (mm ³ /g):	-133.89		
Accessible porosity (%):	12.02		
Inaccessible porosity (%):	-33.75		

ThermoFisher
SCIENTIFIC

SB
Comment

Report date:14-10-14

OTHER CALC.
(Corrected curve)

RESULTS OF TORTUOSITY:

Surface area model:	Cylindrical and Plate
Tortuosity (Camiglia):	2.094
Tortuosity extended calculated:	from Tortuosity
Exponent cylindrical pore:	1.754
Tortuosity extended (Camiglia):	1.664

RESULTS OF PERMEABILITY:

Cylindrical pores permeability (μm ²):	175.72E-6
General permeability calculated:	from Tortuosity
General permeability (μm ²):	167.82E-6

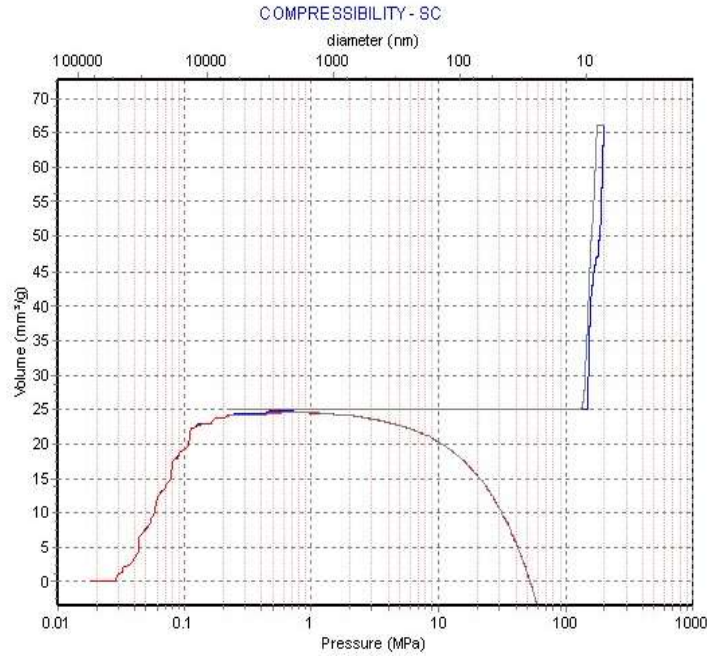
• **Sample C**

ThermoFisher
S C I E N T I F I C

SC
Comment

Report date:14-10-14

COMPRESSIBILITY CORRECTION



RESULTS WITH COMPRESSIBILITY CORRECTION

Correction enabled (Y/N):	Yes		
Linearity range:	From (MPa):	160.6493	To (MPa): 200.8116
Correction factor (mm³/g.MPa)	0.475997		
Compressibility factor (MPa.g/mm³)	2.1009		
Compressed volume (mm³/g):	95.59		
Sample compressibility (1/MPa):	7.197E-3		
Bulk modulus (MPa):	1.389E+2		
Total intruded volume (mm³/g):	-29.45	at pressure (MPa):	200.8116
Intruded vol. (mm³):	4.74		
Envelope density (g/cm³):	2.1491		
Bulk density @ pressure (g/cm³):	2.2644	at pressure (MPa):	0.1735
Apparent density (g/cm³):	2.0212	at pressure (MPa):	200.8116
Real void volume by real dens. (mm³/g):	-284.88		
Accessible porosity (%):	-6.33		
Inaccessible porosity (%):	-54.89		

ThermoFisher
S C I E N T I F I C

SC
Comment

Report date:14-10-14

OTHER CALC.
(Corrected curve)

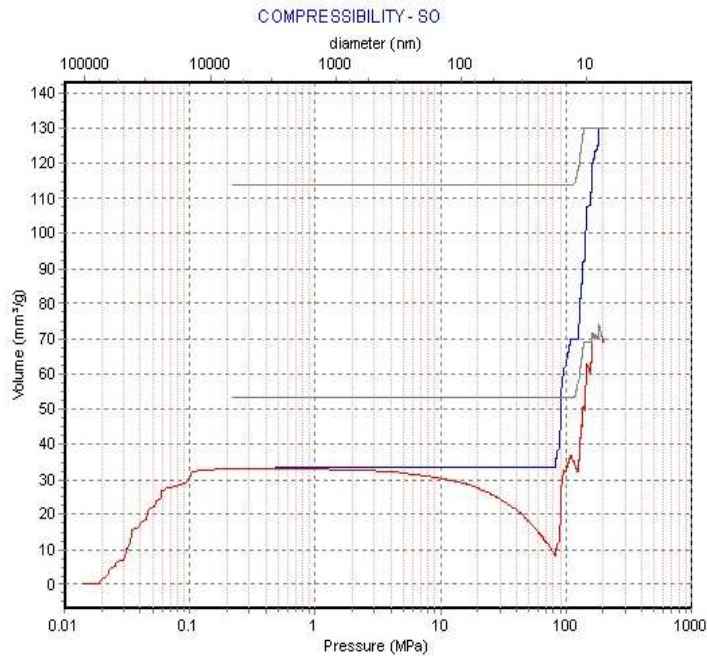
RESULTS OF TORTUOSITY:

Surface area model:	Cylindrical and Plate
Tortuosity (Carniglia):	2.302
Tortuosity extended calculated:	from Tortuosity
Exponent cylindrical pore:	1.754
Tortuosity extended (Carniglia):	1.829

RESULTS OF PERMEABILITY:

Cylindrical pores permeability (µm²):	000E0
General permeability calculated:	from Tortuosity
General permeability (µm²):	167.82E-6

• **Sample O**



RESULTS WITH COMPRESSIBILITY CORRECTION

Correction enabled (Y/N):	Yes		
Linearity range:	From (MPa):	160.6487	To (MPa): 200.8109
Correction factor (mm ³ /g/MPa)	0.303519		
Compressibility factor (MPa.g/mm ³)	3.2947		
Compressed volume (mm ³ /g):	60.95		
Sample compressibility (1/MPa):	2.336E-3		
Bulk modulus (MPa):	4.280E+2		
Total intruded volume (mm ³ /g):	68.95 at pressure (MPa):	200.8109	
Intruded vol. (mm ³):	6.63		
Envelope density (g/cm ³):	1.6844		
Bulk density @ pressure (g/cm ³):	1.7839	at pressure (MPa):	0.1735
Apparent density (g/cm ³):	1.9057	at pressure (MPa):	200.8109
Real void volume by real dens. (mm ³ /g):	-156.50		
Accessible porosity (%):	11.61		
Inaccessible porosity (%):	-37.97		

OTHER CALC.
(Corrected curve)

RESULTS OF TORTUOSITY:

Surface area model:	Cylindrical and Plate
Tortuosity (Carniglia):	2.099
Tortuosity extended calculated:	from Tortuosity
Exponent cylindrical pore:	1.754
Tortuosity extended (Carniglia):	1.668

RESULTS OF PERMEABILITY:

Cylindrical pores permeability (μm ²):	988.97E-7
General permeability calculated:	from Tortuosity
General permeability (μm ²):	942.43E-7

- **Sample 1**

ThermoFisher
S C I E N T I F I C

S1
Comment

Report date:29-10-14

COMPRESSIBILITY CORRECTION



RESULTS WITH COMPRESSIBILITY CORRECTION

Correction enabled (Y/N):	Yes		
Linearity range:	From (MPa):	160.6492	To (MPa): 200.8115
Correction factor (mm³/g.MPa)	0.344142		
Compressibility factor (MPa.g/mm³)	2.9058		
Compressed volume (mm³/g):	69.11		
Sample compressibility (1/MPa):	4.034E-3		
Bulk modulus (MPa):	2.479E+2		
Total intruded volume (mm³/g):	16.21 at pressure (MPa):	200.8115	
Intruded vol. (mm³):	11.89		
Envelope density (g/cm³):	1.2618		
Bulk density @ pressure (g/cm³):	1.3765	at pressure (MPa):	0.4012
Apparent density (g/cm³):	1.2882	at pressure (MPa):	200.8115
Real void volume by real dens. (mm³/g):	14.88		
Accessible porosity (%):	2.05		
Inaccessible porosity (%):	-0.17		

ThermoFisher
S C I E N T I F I C

S1
Comment

Report date:29-10-14

OTHER CALC.
(Corrected curve)

RESULTS OF TORTUOSITY:

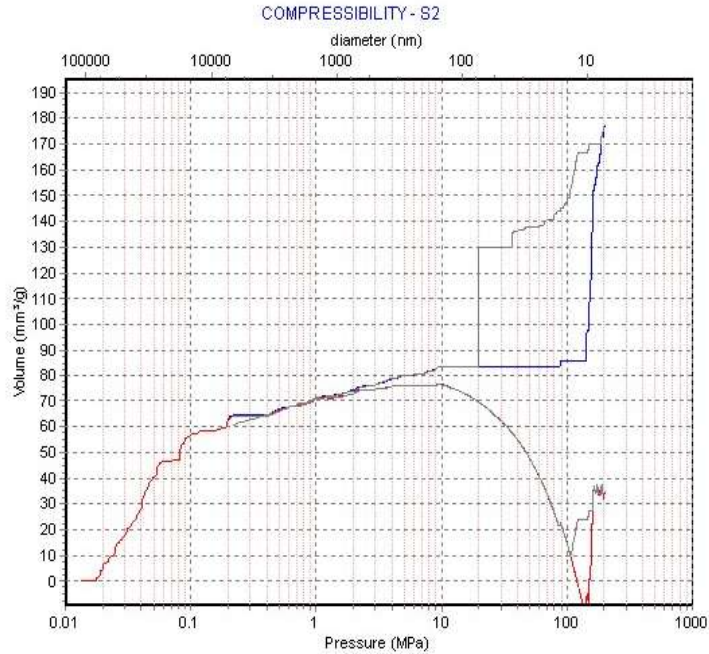
Surface area model:	Cylindrical and Plate
Tortuosity (Carniglia):	2.207
Tortuosity extended calculated:	from Tortuosity
Exponent cylindrical pore:	1.754
Tortuosity extended (Carniglia):	1.754

RESULTS OF PERMEABILITY:

Cylindrical pores permeability (µm²):	000E0
General permeability calculated:	from Tortuosity
General permeability (µm²):	337.93E-4

- **Sample 2**

COMPRESSIBILITY CORRECTION



RESULTS WITH COMPRESSIBILITY CORRECTION

Correction enabled (Y/N):	Yes	
Linearity range:	From (MPa): 160.4892	To (MPa): 200.6115
Correction factor (mm ³ /g.MPa)	0.710882	
Compressibility factor (MPa.g/mm ³)	1.4067	
Compressed volume (mm ³ /g):	142.61	
Sample compressibility (1/MPa):	4.009E-3	
Bulk modulus (MPa):	2.494E+2	
Total intruded volume (mm ³ /g):	34.69 at pressure (MPa):	200.6115
Intruded vol. (mm ³):	11.56	
Envelope density (g/cm ³):	1.0939	
Bulk density @ pressure (g/cm ³):	1.1765	at pressure (MPa): 0.4012
Apparent density (g/cm ³):	1.1370	at pressure (MPa): 200.6115
Real void volume by real dens. (mm ³ /g):	136.59	
Accessible porosity (%):	3.79	
Inaccessible porosity (%):	11.15	

OTHER CALC.
(Corrected curve)

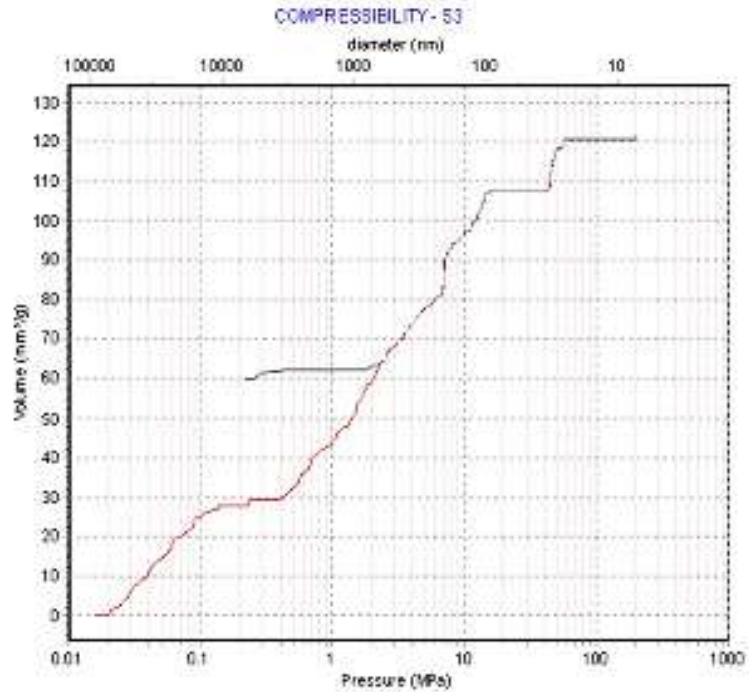
RESULTS OF TORTUOSITY:

Surface area model:	Cylindrical and Plate
Tortuosity (Carniglia):	2.187
Tortuosity extended calculated:	from Tortuosity
Exponent cylindrical pore:	1.754
Tortuosity extended (Carniglia):	1.738

RESULTS OF PERMEABILITY:

Cylindrical pores permeability (μm ²):	513.15E-6
General permeability calculated:	from Tortuosity
General permeability (μm ²):	469.25E-6

- Sample 3



RESULTS WITH COMPRESSIBILITY CORRECTION

Correction enabled (Y/N)	Yes		
Linearity range:	From (MPa):	160.7266	To (MPa): 200.9106
Correction factor (mm ³ /g MPa)	0.002174		
Compressibility factor (MPa g/mm ³)	459.9863		
Compressed volume (mm ³ /g)	0.44		
Sample compressibility (1/MPa)	1.784E-5		
Bulk modulus (MPa)	5.606E+4		
Total intruded volume (mm ³ /g)	121.43	at pressure (MPa):	200.9106
Intruded vol. (mm ³):	5.33		
Envelope density (g/cm ³):	1.3659		
Bulk density @ pressure (g/cm ³):	1.4235	at pressure (MPa):	0.4012
Apparent density (g/cm ³):	1.6375	at pressure (MPa):	200.9106
Real void volume by real dens. (mm ³ /g)	-45.50		
Accessible porosity (%):	16.59		
Inaccessible porosity (%):	-22.80		

OTHER CALC.
 (Corrected curve)

RESULTS OF TORTUOSITY:

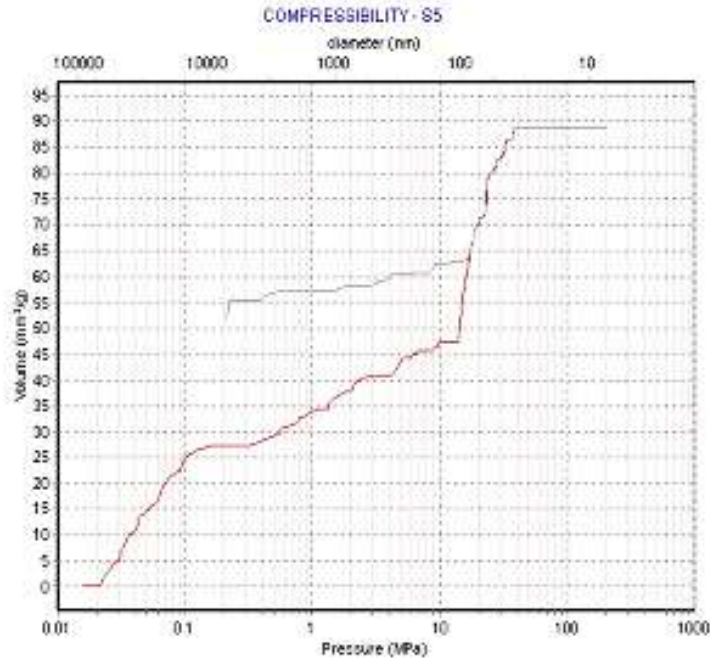
Surface area model	Cylindrical and Plate
Tortuosity (Cariglia):	2.043
Tortuosity extended calculated:	from Tortuosity
Exponent cylindrical pore:	1.754
Tortuosity extended (Cariglia):	1.623

RESULTS OF PERMEABILITY:

Cylindrical pores permeability (μm ²):	112.63E-4
General permeability calculated:	from Tortuosity
General permeability (μm ²):	110.28E-4

• Sample 5

COMPRESSIBILITY CORRECTION



RESULTS WITH COMPRESSIBILITY CORRECTION

Correction enabled (Y/N):	Yes		
Linearity range:	From (MPa): 160.7295	To (MPa): 200.9119	
Correction factor (mm³/g MPa):	0.000000		
Compressibility factor (MPa g/mm³):	0.0000		
Compressed volume (mm³/g):	0.00		
Sample compressibility (1/MPa):	0.000E+0		
Bulk modulus (MPa):	0.000E+0		
Total intruded volume (mm³/g):	88.77 at pressure (MPa): 200.9119		
Intruded vol. (mm³):	5.11		
Envelope density (g/cm³):	1.2292		
Bulk density @ pressure (g/cm³):	1.2736	at pressure (MPa): 0.4012	
Apparent density (g/cm³):	1.3797	at pressure (MPa): 200.9119	
Real void volume by real dens. (mm³/g):	35.94		
Accessible porosity (%):	10.91		
Inaccessible porosity (%):	-6.49		

OTHER CALC.
(Corrected curve)

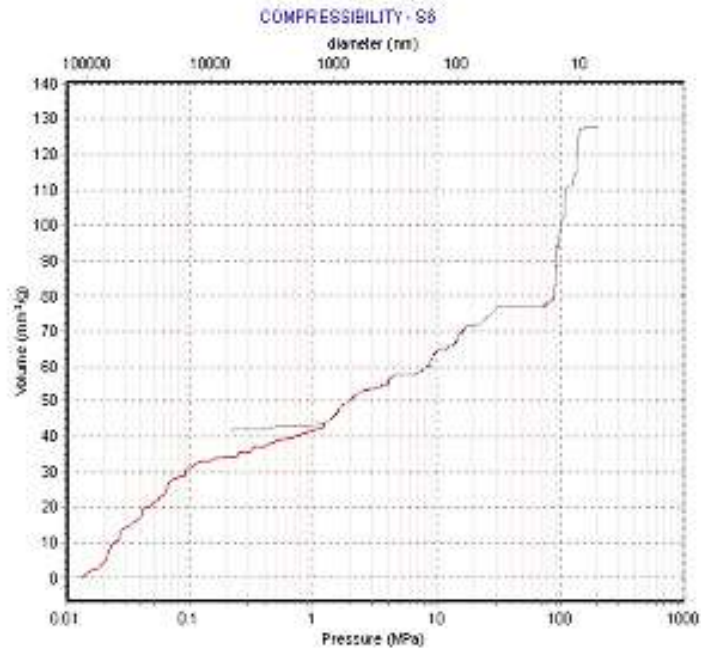
RESULTS OF TORTUOSITY:

Surface area model:	Cylindrical and Plate
Tortuosity (Cariglia):	2.107
Tortuosity extended calculated:	from Tortuosity
Exponent cylindrical pore:	1.754
Tortuosity extended (Cariglia):	1.674

RESULTS OF PERMEABILITY:

Cylindrical pores permeability (µm²):	673.56E-5
General permeability calculated:	from Tortuosity
General permeability (µm²):	639.45E-5

- Sample 6



RESULTS WITH COMPRESSION CORRECTION

Correction enabled (Y/N):	Yes		
Linearity range:	From (MPa):	160.6490	To (MPa): 200.8112
Correction factor (mm³/g MPa):	0.000000		
Compressibility factor (MPa.g/mm³):	0.0000		
Compressed volume (mm³/g):	0.00		
Sample compressibility (1/MPa):	0.000E+0		
Bulk modulus (MPa):	0.000E+0		
Total intruded volume (mm³/g):	127.66	at pressure (MPa):	200.8112
Intruded vol. (mm³):	6.75		
Envelope density (g/cm³):	1.3746		
Bulk density @ pressure (g/cm³):	1.4493	at pressure (MPa):	0.4012
Apparent density (g/cm³):	1.6671	at pressure (MPa):	200.8112
Real void volume by real dens. (mm³/g):	-50.10		
Accessible porosity (%):	17.55		
Inaccessible porosity (%):	-24.43		

OTHER CALC.
 (Corrected curve)

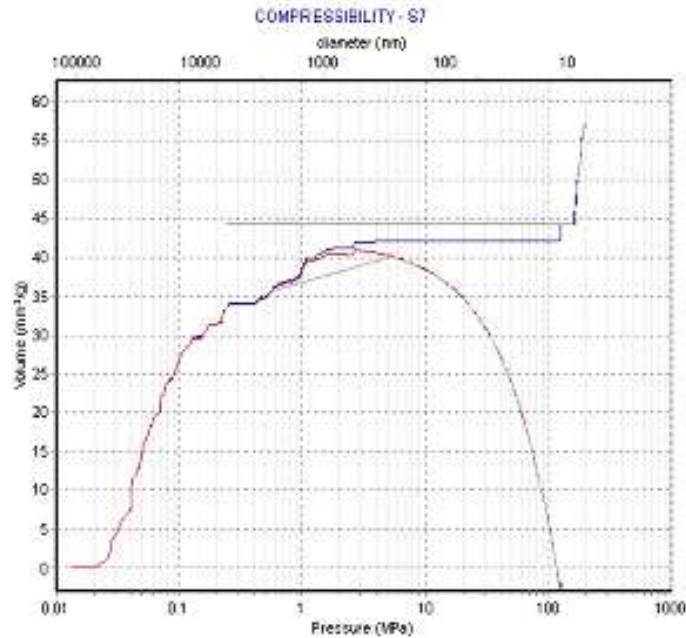
RESULTS OF TORTUOSITY:

Surface area model:	Cylindrical and Plate
Tortuosity (Cariglia):	2.032
Tortuosity extended calculated:	from Tortuosity
Exponent cylindrical pore:	1.754
Tortuosity extended (Cariglia):	1.615

RESULTS OF PERMEABILITY:

Cylindrical pores permeability (µm²):	551.29E-6
General permeability calculated:	from Tortuosity
General permeability (µm²):	542.68E-6

- Sample 7



RESULTS WITH COMPRESSIBILITY CORRECTION

Correction enabled (Y/N):	Yes		
Linearity range:	From (MPa):	160.4092	To (MPa): 200.5115
Correction factor (mm ³ /g MPa):	0.362094		
Compressibility factor (MPa g/mm ³):	2.7617		
Compressed volume (mm ³ /g):	72.60		
Sample compressibility (1/MPa):	6.353E-3		
Bulk modulus (MPa):	1.574E+2		
Total intruded volume (mm ³ /g):	-15.61	at pressure (MPa):	200.5115
Intruded vol. (mm ³):	6.10		
Envelope density (g/cm ³):	1.4271		
Bulk density @ pressure (g/cm ³):	1.4396	at pressure (MPa):	0.4012
Apparent density (g/cm ³):	1.3960	at pressure (MPa):	200.5115
Real void volume by real dens. (mm ³ /g):	-76.66		
Accessible porosity (%):	-2.23		
Inaccessible porosity (%):	-8.74		

OTHER CALC.
(Corrected curve)

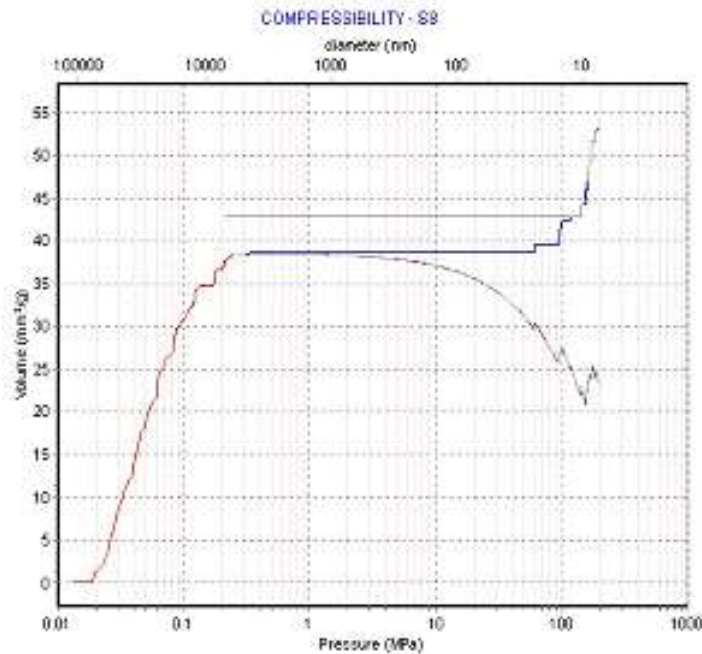
RESULTS OF TORTUOSITY:

Surface area model:	Cylindrical and Plate
Tortuosity (Cariglia):	2.255
Tortuosity extended calculated:	from Tortuosity
Exponent cylindrical pore:	1.754
Tortuosity extended (Cariglia):	1.792

RESULTS OF PERMEABILITY:

Cylindrical pores permeability (μm ²):	000E0
General permeability calculated:	from Tortuosity
General permeability (μm ²):	542.68E-6

- Sample 8



RESULTS WITH COMPRESSIBILITY CORRECTION

Correction enabled (Y/N)	Yes	
Linearity range:	From (MPa): 160.6491	To (MPa): 200.8114
Correction factor (mm³/g MPa)	0.148854	
Compressibility factor (MPa g/mm³)	6.7180	
Compressed volume (mm³/g)	29.89	
Sample compressibility (1/MPa)	2.810E-3	
Bulk modulus (MPa):	3.559E+2	
Total intruded volume (mm³/g):	23.08 at pressure (MPa):	200.8114
Intruded vol. (mm³):	6.93	
Envelope density (g/cm³):	1.1127	
Bulk density @ pressure (g/cm³):	1.1625	at pressure (MPa): 0.4012
Apparent density (g/cm³):	1.1420	at pressure (MPa): 200.8114
Real void volume by real dens. (mm³/g):	121.12	
Accessible porosity (%):	2.57	
Inaccessible porosity (%):	10.91	

OTHER CALC.
(Corrected curve)

RESULTS OF TORTUOSITY:

Surface area model:	Cylindrical and Plate
Tortuosity (Cariglia):	2.201
Tortuosity extended calculated:	from Tortuosity
Exponent cylindrical pore:	1.754
Tortuosity extended (Cariglia):	1.749

RESULTS OF PERMEABILITY:

Cylindrical pores permeability (µm²):	000E0
General permeability calculated:	from Tortuosity
General permeability (µm²):	542.68E-6